Recent Advances in Photocatalytic Removal of Microplastics: Mechanisms, Kinetic Degradation, and Reactor Design

Wael Hamd[1*], Elie A. Daher[2], Tajkia Syeed Tofa[3] and Joydeep Dutta[4*]

[1] Chemical Engineering Department, Faculty of Engineering, University of Balamand, El-Koura, Lebanon, [2] Petrochemical Engineering Department, Faculty of Engineering III, Scientific Research Center in Engineering (CRSI), Lebanese University, Hadat, Lebanon, [3] Department of Civil Engineering (CE), Military Institute of Science and Technology (MIST), Mirpur Cantonment, Dhaka, Bangladesh, [4] Functional Materials, Department of Applied Physics, School of Engineering Sciences, KTH Royal Institute of Technology, Stockholm, Sweden

Plastic products are used in almost all aspects of our daily life. Due to their low cost, portability, durability, and resistance to degradation, these products are affecting the health of the environment and biota on a global scale. Thus, the removal and mineralization of microplastics is an important challenge in the 21st century. Advanced oxidation processes (AOPs) have recently been identified as a viable treatment technique for tackling recalcitrant organic molecules and polymers. However, information on kinetic degradation mechanisms and photocatalytic reactor design is insufficient. This review discusses the fundamentals of photocatalysis and photo-Fenton processes in addition to the photocatalytic degradation mechanisms. We also introduce different characterization techniques of the major microplastic pollutants such as PE, PP, PVC, PS, PMMA, and PA66. In addition, a detailed overview of the major existing photocatalytic plants and the scaling-up methods of photoreactors are discussed.

Keywords: microplastics, advanced oxidation processes, photocatalysis, microplastics characterization, photocatalytic reactor design, reactor upscaling

1 INTRODUCTION

It is rare to experience similar growth in production and usage as the plastics industry has done in the span of 60 years, plasticizing the modern world, and justifiably dubbing the 20th and 21st centuries the "Plastics Age" (Porta, 2021).

By the middle of the 19th century, and in the wake of industrialized goods production, inventors were attempting to tackle a new economic problem, resulting from the increasing scarcity of natural-derived materials. It was then that the first synthetic polymer was produced by John Wesley Hyatt around 1869 from the treatment of cellulose polymer and camphor (Evode et al., 2021). As research progressed, the dawn of the 20th century witnessed the production of the "Bakelite", the first synthetic plastic, by Leo Hendrik Baekeland in 1907 (Geyer et al., 2017). Owing to its remarkable versatility and utility, plastics went into large-scale production to accompany the technological revolution that followed the beginning of the so-called post-World War II in what was

known as the "Great Acceleration of population, industry and resource utilization" (Porta, 2021). Today, plastics and plastic-based materials are produced in millions of tons at a rate exceeding two hundred million tons per annum (Nabi et al., 2021). Plastic fabrication is expected to increase twofold in the next 20 years if current trends continue (Lebreton and Andrady, 2019).

However, plastics, the wonder material of the 1960s, became a victim of its own success. As a result of the huge production and inefficient waste management practices, plastic debris has progressively invaded the environment from the poles to the equator, and from the depths of the oceans to the tops of mountains, jeopardizing the aquatic and terrestrial ecosystem (Browne et al., 2010). As of 2015, it is appraised that only about 9% of the 6,300 Mt of produced plastic litter was recycled, 12% was incinerated, and 79% was dumped in landfills or the natural environment (Geyer et al., 2017). Over 5 trillion pieces of plastic, weighing over 260,000 tons, are now hovering over the ocean's surface (Eriksen et al., 2014). If current production and waste management trends continue, by 2050, plastics are anticipated to account for up to 54 wt% of all discharged anthropogenic leftover into the environment, with 12,000 Mt ending up in landfills or aquatic media (Geyer et al., 2017; Cao et al., 2021). Plastics are a versatile material made up of long-chain synthetic polymers with tenacious characteristics, mainly processed from petroleum-based products, and consuming approximately 1.6 billion L of oil annually (Knoblauch et al., 2018). Recent studies estimated that plastic production would require in the next 30 years roughly 20% of petroleum products consumed globally and would account for 15% of the annual carbon emissions (Lebreton and Andrady, 2019).

Plastics pollutants are broadly defined into five categories depending on their dimensions: megaplastics (over 1 m), macroplastics (below 1 m), mesoplastics (below 2.5 cm), microplastics (MPs) (below 5 mm), and nanoplastics (under 1 μm) (Thompson et al., 2004; Wright et al., 2013; Law and Thompson, 2014; Wang et al., 2017). Within this scope and since 2004, the term "microplastics" has been popularly adopted by scientists and environmentalists (Hartmann et al., 2019). More recently, MPs are termed as "synthetic solid plastic particle or polymeric matrix with regular or irregular shapes and a size ranging from 1 μm to 5 mm" (Frias and Nash, 2019).

Following their unabated discharge, MPs have been found in seawater, coasts (Zhou et al., 2016), estuarine sediments (Qiu et al., 2015), rivers (Sanchez et al., 2014), lakes (Wang et al., 2017), soils (Zhou et al., 2019), and air (Abbasi et al., 2018), among others, outnumbering the large portion of plastic debris (Hale et al., 2020). Moreover, these small invaders are of great environmental concern, especially due to their size; it is accessible to a wide range of organisms, starting from the smallest species such as zooplankton to the bigger ones, with potential physical and toxicological issues (Law and Thompson, 2014; Hodson et al., 2017; He et al., 2018).

Due to their small size, ingested MPs can circulate throughout the food web up to the food chains of human consumers (Revel et al., 2018). According to reports, a human being could consume between 39,000 and 52,000 MPs per year through food and beverages, while 4,000 MPs to 90,000 MPs could be added annually if tap and bottled water are respectively consumed (Cox et al., 2019). Recent studies suggest that MPs of micrometer size or smaller could adversely affect human health (Rist et al., 2018; Chen et al., 2020).

Conventional wastewater treatment plants (WWTPs) were found to be ineffective when it comes to MPs removal. These MPs are barely detectable on the macroscopic scale, and can easily escape capture by WWTPs ultimately ending up in the aquatic environment (Murphy et al., 2016; Lasee et al., 2017). Following the water treatment *via* WWTPs and drinkable water treatment plants (DWTPs), a ~70% removal efficiency of microfibers (MPFs) was only achieved, with treated wastewater containing up to ~347 of undetected MPFs/L (Sol et al., 2021). Furthermore, studies about WWTPs from different locations revealed an abundance of MPs in the treated water between 5.00×10^{5} and 1.39×10^{10} particles on a daily basis (Liu et al., 2021).

The failure of conventional WWTPs to effectively remove MPs explains the carried-out efforts by scientists and engineers to develop suitable innovative technologies capable of treating these particles and neutralizing their harmful effects. In this regard, technologies for removing MPs, including physical, chemical, and biological treatments, were developed (Mumford et al., 2012; Talvitie et al., 2017; Ziajahromi et al., 2017; Sun et al., 2019). However, these methods show some main drawbacks (see **Figure 1**), such as the further required treatment of resulting sludge (Kim et al., 2022), production of secondary MPs, and non-reusability, making them unattractive to be employed for tackling the MPs in the environment (Dey et al., 2021).

In order to overcome these restraints, it was vital to search for more advanced and efficient technologies.

FIGURE 1 | Drawbacks of some of the MPs removal technologies.
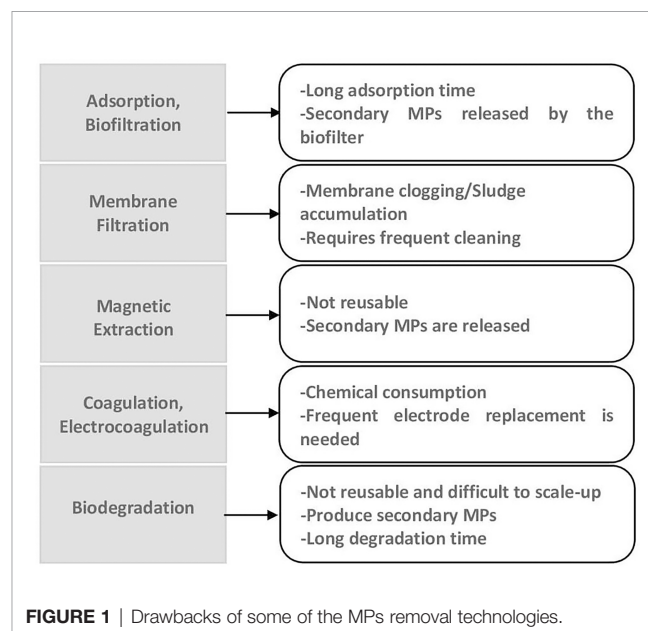
In this view, advanced oxidation processes (AOPs) are considered environmental-friendly methods and were proposed as tertiary treatment for different types of wastewater effluents owing to their versatility and ability to remove non-biodegradable and chemically stable pollutants (Konstas and Konstantinou, 2019; Zhang et al., 2019; Antonopoulou et al., 2021). The principle of AOPs is based on physicochemical transformations that result in molecular disintegration, simplification of the chemical structure, and finally mineralization. Such processes involve the formation of highly reactive radical species involving the hydroxyl ($HO^{\bullet}$), superoxide (O_2^-), hydroperoxyl (HO_2), alkoxyl ($RO^{\bullet}$), sulfate (SO_4^-) and chlorine ($Cl^{\bullet}$) radicals (Vione et al., 2014; Potakis et al., 2017; Alfaifi et al., 2018). A general classification of the AOPs is shown in **Figure 2**.

Among AOPs, photocatalysis and Fenton processes show a relatively high degradation rate and efficiency, making them a promising alternative for degrading various recalcitrants like MPs (Mokhbi et al., 2019; Kim et al., 2022). Yet, the employment of these techniques at an industrial scale remains very challenging due to the interference of several parameters that could affect the degradation process such as (i) the type and size of MPs, (ii) the light source and its intensity, in addition to (iii) the design of the photoreactor. Therefore, this work reviews, in an extensive manner, recent advances in photocatalysis technology, mechanism, and kinetics of MPs photodegradation, as well as the upscaling of photocatalytic reactors.

2 RECENT ADVANCES IN PHOTOCATALYSIS TECHNOLOGY

2.1 Fundamentals of Photocatalysis

This technology could fall into two primary subgroups: homogeneous and heterogeneous photocatalytic systems.

Homogeneous systems are broadly employed due to their high reaction rate, short process time, and high accessibility, yet they present some critical drawbacks such as high cost, cumbersome extraction, complicated recycling procedures, and reactor corrosion (Ali et al., 2014; Cui et al., 2018). Moreover, implementing process-engineering strategies in photocatalytic processes favors heterogeneous photocatalysis due to the higher stability and ease of recovering heterogeneous photocatalysts.

Generally, photocatalysts are semiconductor (SC) materials that are photoactive. When an SC is irradiated by a light source of photonic energy (hv) larger than that of its bandgap (E_{bg}), an excited electron shifts from the valence band (VB) to the vacant conduction band (CB), and an electron (e^-)–hole (h^+) pair is created (Zhang et al., 2018). Consequently, the nature of the light source critically affects the concentration of (e^-)–(h^+) pairs and therefore the effectiveness of the system. Regardless of the type of pollutants, molecules, or MPs particles, the principle of photocatalytic degradation is quite similar and mainly grounded on the oxidation by ROS to transform the toxic product into less harmful components (Kim et al., 2022). The steps of such a mechanism are explained in **Figure 3**. As seen, while a part of the photo-generated electron–holes (1) recombine within 10 to 100 ns through radiative (photoluminescence) or non-radiative (energy release) processes (5), the rest generate a charge carrier capable of spatially separating on the catalytic surface (2) (Alfaifi et al., 2018; Hoffmann et al., 1995 Habib et al., 2020; Danish et al., 2021).

Upon reaching the surface, these electron–hole pairs could either recombine again (6) or undergo electronic transfers with the localized states of the adsorbed molecules (3),(4). In this regard, the protons' reduction [E_{NHE} (H^+/H_2) = 0.0 eV] and water oxidation [E_{NHE} (O_2/H_2O) = 1.23 eV] are the main reference energy levels that acquire a particular relevance concerning most SCs (as seen in **Figure S1**) (Tong et al., 2012).

Generally, metal oxide SCs have their valence bands with the main contribution from oxygen 2p orbitals, at 1–3 eV below the
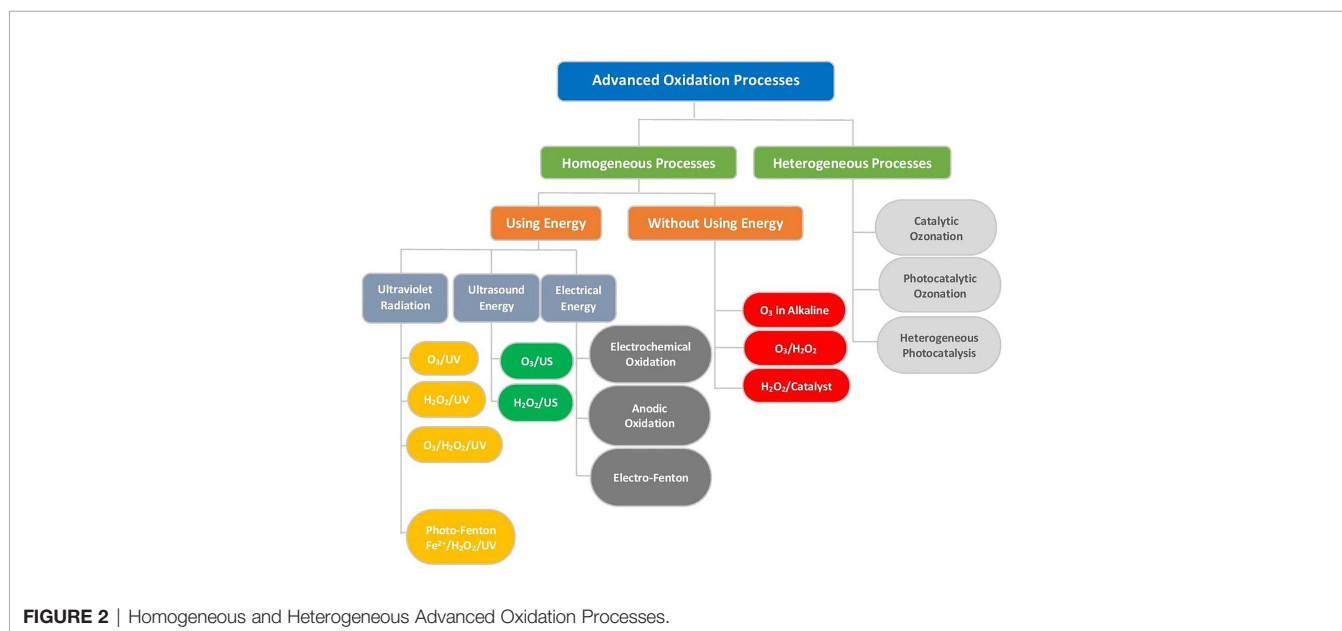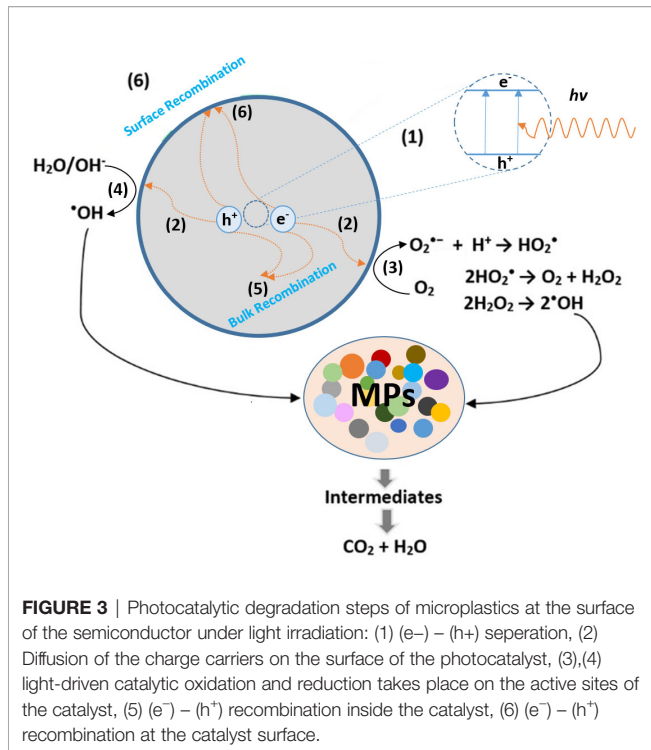

FIGURE 2 | Homogeneous and Heterogeneous Advanced Oxidation Processes.

FIGURE 3 | Photocatalytic degradation steps of microplastics at the surface of the semiconductor under light irradiation: (1) (e−) – (h+) seperation, (2) Diffusion of the charge carriers on the surface of the photocatalyst, (3),(4) light-driven catalytic oxidation and reduction takes place on the active sites of the catalyst, (5) (e$^-$) – (h$^+$) recombination inside the catalyst, (6) (e$^-$) – (h$^+$) recombination at the catalyst surface.

O_2/H_2O redox couple, while transition metal oxides with conduction bands mainly constituted by d orbitals of the metal have the position of their s orbital close to, or below the H_2O reduction potential (Coronado, 2013). Thus, in aqueous media, a photo-activated SC enables the generation of reactive oxygen species (ROS) such as hydroxyl radical ($^\bullet$OH) and superoxide radical ($O_2^{\cdot-}$), which exhibit strong oxidation of organic matters, leading to the total mineralization of recalcitrant organic particles into less harmful products such as H_2O and CO_2 (Ganguly et al., 2019; Habib et al., 2020; Saravanan et al., 2020).

SC photocatalysts can be classified into three main categories: single, double (binary), and three (ternary) components (**Figure 4**). The usage of classical single components shows certain limits related to the large amount of electron–hole recombination, low absorption of the visible region, and poor conduction of the charge carrier (Pawar and Lee, 2015). Although binary and ternary photocatalysts have been showing a better performance compared to the single components, they present many downsides when used alone (Xu et al., 2019).

For instance, SCs with sulfides or nitrides (binary SC) possess a narrow bandgap but are unstable in the aqueous medium (Mishra and Chun, 2015). Moreover, using metal oxides in their pure form presents limited adsorption capacity, lower recovery, reusability, and higher recombination rates (Mohamed et al., 2020). For example, TiO_2-based SCs have been studied, and widely used for photocatalytic applications, yet, they present poor quantum yield due to the fast recombination rate of photogenerated electron–hole pairs, poor and selective adsorption, and short-lived photo-generated carriers (Adekoya et al., 2017; Lum et al., 2019). Another broadly used metal oxide, zinc oxide (ZnO), is prone to be soluble in both alkaline and acidic medium (Saravanan et al., 2020). In addition, certain ternary SCs have an enough narrow E_{bg} that renders them active under visible light, yet they do not possess appropriate band edge potentials to perform diverse reactions (Xu et al., 2019). For this reason, optimum formulations of performant photocatalytic systems can be achieved by either coupling large bandgap binary/ternary SCs with narrower bandgap binary/ternary ones, or coupling modified/unmodified SCs into nanocomposites, or even by adopting the two-step photoexcitation system known as Z-scheme (1st, 2nd, and 3rd generations) (Yadav et al., 2018; Xu et al., 2019; Chung et al., 2019).

3 PHOTO-FENTON PROCESS

Fenton oxidation processes, another classic category of AOPs, is one of the most popular and interesting techniques due to its

FIGURE 4 | Flow chart of some binary and ternary semiconductor photocatalysts.
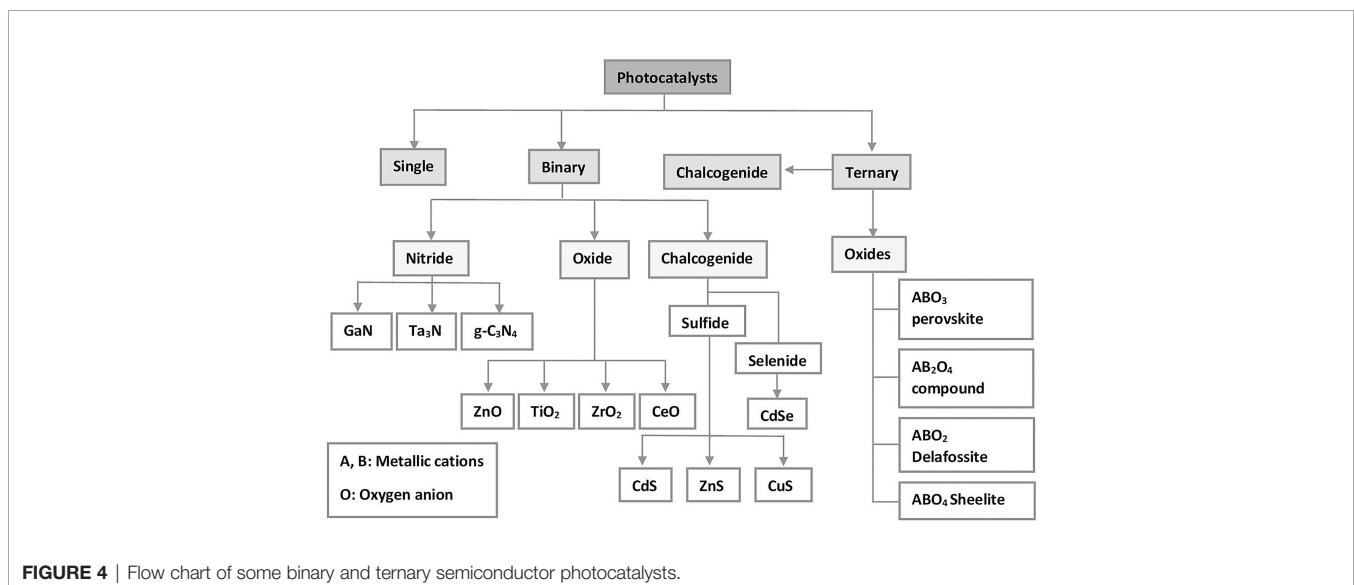
satisfying depuration ability (at room temperature and barometric pressure), a broad spectrum of applications, interference resiliency, procedure simplicity, and quick degradation/mineralization of recalcitrant organics (Hamd and Dutta, 2020). The process was first brought to light by Fenton et al. in 1894 (Fenton, 1894) in its basic form, consisting of the catalytic reaction of H_2O_2 with iron ions (Fe^{2+}) and producing hydroxyl radical ($^\bullet OH$), the second-highest oxidized species with a potential $E°C(OH/H_2O) = +2.8$ Vs NHE as shown in (Rn. 1).

$$Fe^{2+} + H_2O_2 \rightarrow Fe^{3+} + OH^- + {}^\bullet OH \qquad (Rn.\ 1)$$

However, besides the oxidation of Fe^{2+} to Fe^{3+}, the technique requires the generation of the Fe^{2+} species throughout its reduction to Fe^{3+} to generate $^\bullet OH$ (Rn. 2). With the rate of the reduction reaction ~6,000 times lower than that of the oxidation, the efficiency of the oxidation/reduction cycle of Fe(III)/Fe(II) is dramatically hindered and leads to the accumulation of Fe^{3+} in the solution (Song et al., 2006; Martínez-Huitle et al., 2015).
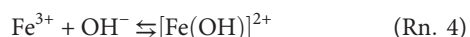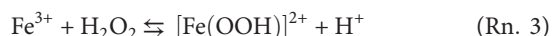
$$Fe^{3+} + H_2O_2 \rightarrow Fe^{2+} + H^+ + HO_2^\bullet \qquad (Rn.\ 2)$$
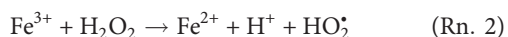
Facing the fact that Fe^{3+} begins to precipitate at >pH = 3 to form the so-called iron sludge (oxyhydroxide) (Xue et al., 2018), which is considered a heavy pollutant, and leads to severe losses of ferric ions in the medium, homogenous Fenton is recommended to be performed in strong acidic medium (Hamd and Dutta, 2020)..

To overcome this inconvenience and to expand the application pH of the technology, various approaches have been adopted such as coupling homogeneous Fenton with UV-vis/solar irradiation, using chelating agents (CAs), or employing heterogeneous Fenton systems (Hamd and Dutta, 2020).

3.1 Coupling of Homogeneous Fenton Process With Light (Photo-Fenton)

The generation of stable hydroxo-iron(III) complexes such as [Fe(OOH)]$^{2+}$ and [Fe(OH)]$^{2+}$ by the interaction of Fe^{3+} ions with H_2O_2 and OH^- results in a poor regeneration of iron(III) ions (Rn. 3,4) (Ahmed et al., 2011):

$$Fe^{3+} + H_2O_2 \leftrightarrows [Fe(OOH)]^{2+} + H^+ \qquad (Rn.\ 3)$$

$$Fe^{3+} + OH^- \leftrightarrows [Fe(OH)]^{2+} \qquad (Rn.\ 4)$$

Herein, this rate could be increased by the introduction of a UV-vis (<580 nm) irradiation source, thus reducing sludge formation and maintaining the oxidation/reduction cycle in a step that produces greater amounts of $^\bullet OH$ radicals (Rn. 5) (Babuponnusami and Muthukumar, 2014; Lee et al., 2014).

$$[Fe(OH)]^{2+} + h\nu \rightarrow Fe^{2+} + {}^\bullet O_2H \quad \lambda < 580\ nm \qquad (Rn.\ 5)$$
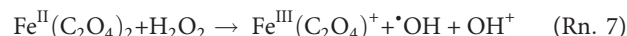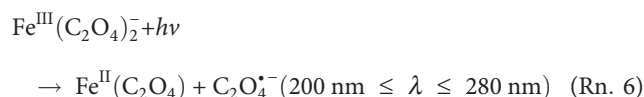
Nevertheless, several key parameters have to be considered including (i) the initial concentration of recalcitrant molecules, (ii) the initial concentration of Fenton reagents, (iii) the operating temperature, and, most critically, (iv) the pH (Hamd and Dutta, 2020). For instance, at pH > 3.5, various aspects are noticed:

- $^\bullet OH$ radicals generation by the decomposition of H_2O_2 is hindered due to the deficiency of H^+ (Walling et al. 1975). (2019).
- H_2O_2 decomposition to water and oxygen is accelerated at pH > 5 (Meeker and United States Patent Office, 1963).
- $^\bullet OH$ radicals' oxidation potential is shrunken as pH values increase (E°C = 2.8–1.95 V at pH 0–14) (Samet et al., 2009).
- Production of ferric oxyhydroxide (FeOOH) at pH > 4 decreases the degradation rate (Tang and Huang, 1996).
- The increased stability of H_2O_2 owing to the generation of $,H_3O_2^+$ blocks the formation of $^\bullet OH$ radicals.

3.1.1 Role of Chelating Agents in Homogeneous Photo-Fenton Processes in Preventing Sludge Formation

To extend the working pH of homogeneous photo-Fenton processes, organic/inorganic ligands known as CAs, e.g., EDTA (ethylenediaminetetraacetic acid), EDDS (ethylenediamine-N, N'-disuccinic acid), oxalate, NTA (nitrilotriacetic acid), CMCD (carboxymethyl β-cyclodextrin), tartrate, citrate, and succinate, are used (Luna et al., 2012). Moreover, various advantages were proved to come along with the usage of CAs, including:
- Increase quantum yield of $^\bullet OH$ radicals.
- Improving Fe^{3+} reduction to Fe^{2+}, resulting in additional $^\bullet OH$ radicals, as shown in the case of oxalate ion (Rn. 6, 7):

$$Fe^{III}(C_2O_4)_2^- + h\nu$$
$$\rightarrow Fe^{II}(C_2O_4) + C_2O_4^{\bullet -} (200\ nm \leq \lambda \leq 280\ nm) \quad (Rn.\ 6)$$

$$Fe^{II}(C_2O_4)_2 + H_2O_2 \rightarrow Fe^{III}(C_2O_4)^+ + {}^\bullet OH + OH^+ \qquad (Rn.\ 7)$$

More interestingly, the usage of CAs such as EDTA is broadly recommended in the heterogeneous photo-Fenton process (detailed in the next section). Adsorption of EDTA on magnetite, for example, could promote Fe_3O_4 dissolution, resulting in an improved catalytic reaction (He et al., 2015). Nevertheless, the high concentration of some of the CAs should be controlled because they may be strongly competing with H_2O_2 species for the boundless active catalytic sites (Huang et al., 2013).

3.2 Heterogeneous Photo-Fenton Processes

The advantage of the heterogeneous photo-Fenton processes relies upon extending the medium pH towards more practical ranges because catalytic reactions take place at the active region on the solid catalyst's surface, therefore reducing the leaching of iron ions, decreasing the production of the iron sludge, and permitting the reusability of the catalyst (Liu et al., 2017; Hamd and Dutta, 2020).
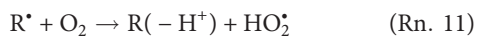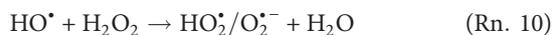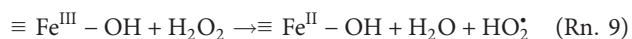
Basically, two main interfacial mechanisms were proposed based on the two-stage degradation kinetic process (**Figure S2**) (He et al., 2015; Hamd and Dutta, 2020):

- Slow induction period mainly consisting of heterogeneous reactions and surface iron leaching (homogeneous reactions).
- Leaching of surface iron (homogeneous reactions), accompanied by quick induction time on the catalyst surface for heterogeneous catalytic reactions.
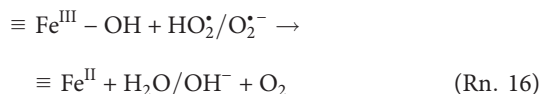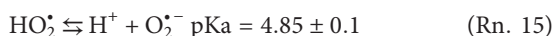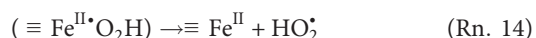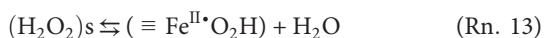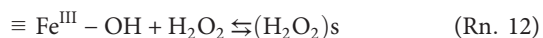
In heterogeneous Fenton systems, hydroxyl radical $^\bullet OH$ (the main oxidant species) is commonly produced either from heterogeneous catalytic reactions between the surficial Fe^{II} ($\equiv Fe^{II}$) and H_2O_2 (Rn. 8) (Lin and Gurol, 1998) or from the outer-sphere reaction of uncomplexed Fe^{2+} ions with H_2O_2 (Rn. 10) (Remucal and Sedlak, 2011):

$$\equiv Fe^{II} + H_2O_2 \rightarrow \equiv Fe^{III} - OH + ^\bullet OH \qquad (Rn.\ 8)$$

As for other oxidants such as hydroperoxyl radical (HO_2) and superoxide anion (O_2^-), they are produced by reactions involving surface-complexed Fe^{III} ($\equiv Fe^{III} - OH$) and H_2O_2, $^\bullet OH$ and H_2O_2, in addition to reactions involving carbon-centered $R^\bullet$ and oxygen (Rn. 9-11) (Santos-Juanes et al., 2011; He et al., 2015).

$$\equiv Fe^{III} - OH + H_2O_2 \rightarrow \equiv Fe^{II} - OH + H_2O + HO_2^\bullet \quad (Rn.\ 9)$$

$$HO^\bullet + H_2O_2 \rightarrow HO_2^\bullet/O_2^{\bullet -} + H_2O \qquad (Rn.\ 10)$$

$$R^\bullet + O_2 \rightarrow R(-H^+) + HO_2^\bullet \qquad (Rn.\ 11)$$

Owing to the proportionality of the catalytic decomposition rate of hydrogen peroxide to its own concentration and the surface area of the goethite as well (Huang et al., 2001; Kwan and Voelker, 2003), the proposed mechanism of H_2O_2 decomposition by Lin and Gurol seems to be the most reasonable (Rn. 12-18) (Lin and Gurol, 1998):

$$\equiv Fe^{III} - OH + H_2O_2 \leftrightarrows (H_2O_2)s \qquad (Rn.\ 12)$$

$$(H_2O_2)s \leftrightarrows (\equiv Fe^{II} \cdot O_2H) + H_2O \qquad (Rn.\ 13)$$

$$(\equiv Fe^{II} \cdot O_2H) \rightarrow \equiv Fe^{II} + HO_2^\bullet \qquad (Rn.\ 14)$$

$$HO_2^\bullet \leftrightarrows H^+ + O_2^{\bullet -} \quad pKa = 4.85 \pm 0.1 \qquad (Rn.\ 15)$$

$$\equiv Fe^{III} - OH + HO_2^\bullet/O_2^{\bullet -} \rightarrow$$
$$\equiv Fe^{II} + H_2O/OH^- + O_2 \qquad (Rn.\ 16)$$

$$^\bullet OH +\equiv^{Fe^{II}} \rightarrow \equiv Fe^{III-} OH \qquad (Rn.\ 17)$$

$$^\bullet OH^+ (H_2O_2)^s \rightarrow^{\equiv} Fe^{III-} OH^+ HO_2^\bullet + H_2 O \qquad (Rn.\ 18)$$

Besides these reactions, coupling the system with solar irradiation, photocatalysis could occur owing to the narrow bandgaps (2.0–2.3 eV) of iron oxide (Gulshan et al., 2010). The introduction of sunlight to heterogeneous photo-Fenton

processes was found to be beneficial compared to UV light sources due to the noticeable decrease in operating expenses and the photolysis of ferric complexes, which takes place at wavelengths of approximately 600 nm and provides the catalytic medium with a higher number of $^\bullet OH$ radicals (Hamd and Dutta, 2020).

4 APPLICATION OF AOPS FOR DEGRADATION OF MICROPLASTICS

Among the AOP techniques, heterogeneous photocatalysis and photo-Fenton process proved to be an efficient means for the removal of MPs present in water. Photocatalytic water treatment has already reached the stage of the industrial pilot. Although the efficacy of the photocatalytic process has been well established in families of very different organic compounds such as dyes (Guillard et al., 2003; Saggioro et al., 2015; Berkani et al., 2020), pesticides (Herrmann and Guillard, 2000; Kaur and Kaur, 2021), saturated/unsaturated hydrocarbons (Herrmann, 1999; Ul haq et al., 2020), and phenols (Liao et al., 2009; Wang et al., 2009; Mozia et al., 2012; Mohamed et al., 2020), the application of photocatalysis for the treatment of micro- and nano-plastics has been attempted for just a few years. For instance, Tian et al. (2019) conducted a photocatalytic degradation of polystyrene (PS) nanoplastics in water and air mediums under a 254-nm irradiation source utilizing (Hartmann et al., 2019) C radioisotope tracer technology (Tian et al., 2019). PS nanoplastics mineralized more readily in water ($17.1 \pm 0.55\%$) than in air ($6.17 \pm 0.1\%$), proving the importance of the aqueous medium in improving the photo-transformation of the PS nanoplastics. Recently, Nabi et al. (2020) carried out a photocatalytic degradation of PS microspheres in addition to polyethylene (PE), over TiO_2 nanoparticle films under an ultraviolet irradiation source (Nabi et al., 2020). After 12 h, a TiO_2 nanoparticle film produced with Triton X-100 demonstrated near-complete mineralization (98.40%) of 400-nm PS and a significant photodegradation rate of PE after 36 h, resulting in CO_2.

Li et al. (2020) used a polypyrrole/TiO_2 (PPy/TiO_2) nanocomposite as a photocatalyst to degrade PE plastic under sunlight irradiation (Li et al., 2020). The photocatalyst was synthesized using sol-gel and emulsion polymerization processes. They discovered that exposing PE plastic to solar radiation for 240 h lowered its weight by 35.4% and 54.4% of Mw, respectively. The degradation of PE was attributed to the strong existing interaction between the interface of PE and PPy/TiO_2 photocatalyst as demonstrated by FTIR spectroscopic studies. Ariza-Tarazona et al. (2019) used N-TiO_2 exposed to visible light to photocatalyze the breakdown of genuine samples of HDPE MPs isolated from a commercial facial cleanser (Ariza-Tarazona et al., 2019). The photocatalyst showed a high capacity for mass loss of HDPE MPs in both solid and aqueous environments. It was also demonstrated that the ambient conditions, interactions between pollutants and photocatalyst, and the catalytic surface area should all be properly established

or tailored to avoid photocatalyst deactivation. Lee et al. (2020) carried out a photocatalytic degradation of polyamides microfibers PA66 over different TiO_2 doses (Lee et al., 2020). With the employment of 100 mg of TiO_2/L, the degradation efficiency reached its optimum under UVC irradiation, and PA66 microfibers lost 97% of their mass (in 48 h). These photocatalytic conditions produced a modest level of by-products (less than 10 mg/L COD). As a result, photocatalysis using TiO_2 and UVC could be a viable option for treating microfibers in WWTPs. Furthermore, we have recently published in Dutta's group two interesting papers about the photocatalytic degradation of PE films and PP beads in water flow. In the first work, Tofa et al. (2019) used visible-light-triggered heterogeneous zinc oxide photocatalysts to successfully degrade a 1 cm × 1 cm low-density polyethylene (LDPE) film (Tofa et al., 2019).. The carbonyl index of residues increased by 30%, as did the brittleness, which was accompanied by a high number of wrinkles, cracks, and cavities on the surface. The oxidation degree turned out to be directly proportional to the catalytic surface area. In another work, Uheida et al. (2020) suggested a unique MPs removal approach that uses coated glass fiber substrates with ZnO photocatalyst to trap low-density polypropylene (PP) (Uheida et al., 2020). Irradiating PP MPs for 2 weeks with visible light resulted in a 65% reduction in mean particle volume. GC/MS was used to identify the primary photodegradation by-products, which were determined to be predominantly harmless compounds. Finally, Colburn et al. (2020) suggested a new idea for MPs removal by introducing beforehand a 2 wt% catalyst anatase TiO_2 to the HDPE or LDPE films during their synthesis (Colburn et al., 2020). Photo degradation under ambient conditions and solar irradiations could be a scalable and cost-effective defense strategy against plastic litter. A summary of some appealing works published in the last two decades is chronologically presented in **Table 1**.

On the other hand, Fenton's reagent method also has a very positive influence on the treatment process, especially for non-degradable organic pollutants. Fenton's reagent removes or degrades a wide variety of contaminants in an aqueous solution either alone or in combination with other processes. Fenton process was successfully used in textile (Arslan-Alaton et al., 2007; Liu et al., 2007; Nadeem et al., 2020), pharmaceutical (Martínez et al., 2003; Molina et al., 2020), dyeing (Gulkaya et al., 2006; Wang, 2008; Salgado et al., 2020), olive oil mills (Rivas et al., 2001; Beltrán-Heredia et al., 2001; RuÄz-Delgado et al., 2020), oil (Sivagami et al., 2019; Gamaralalage et al., 2019), and cosmetics industries (Bautista et al., 2007; De Andrade et al., 2020), as well as in the reduction of polynuclear aromatic hydrocarbons (Beltrán et al., 1998; Singa et al., 2021), the treatment of brines (Rivas et al., 2003), the degradation of phenol and bisphenols (Carriazo et al., 2005; Zulfiqar et al., 2021), the treatment of effluent from herbicides and pesticides production industry (Sangami and Manu, 2017; Zhao and Zhang, 2021), the treatment of landfill leachates (Tejera et al., 2021; Filho et al., 2021), the degradation of recalcitrant oil spill components anthracene and pyrene (Sekar and DiChristina, 2017; RuÄz-Delgado et al., 2020), the inactivation of

Escherichia coli K12 (Rivas et al., 2001), the treatment of recalcitrant industrial wastewater (Cai et al., 2021), and the treatment of high-molecular-weight melanoidin molecules (Raji et al., 2021). More details about Fenton technology for the treatment of recalcitrant organic molecules in several industries can be checked out in our recently published book chapter (Hamd and Dutta, 2020).

In addition, the Fenton process was also used for tackling MPs: After 6 h of potentiostatic electrolysis at −0.7 V vs. Ag/AgCl at 100°C, Miao et al. (2020) demonstrated that an EF-like technique based on TiO_2/C cathode was successfully used to degrade PVC MPs with 56 wt% elimination and 75% dechlorination efficiency (Miao et al., 2020). As a result, this method offers a viable and environmentally benign strategy for the degradation of PVC MPs, with the potential to be extended to additional chlorinated species of plastics such as 2,4-dichlorophenol, PE, PP, and PS. Moreover, Liu et al. (2019) showed a significant fragmentation of PS and PE MPs during the oxidation processes by $K_2S_2O_8$ and after Fenton treatment (Liu et al., 2019). After 30 days of heat-activated $K_2S_2O_8$ treatment, the sizes of almost all MPs were decreased from 40–50 μm to <30 μm and 80.1% and 97.4% of PS and PE were below 20 μm, respectively. The fragmentation processes and the degradation rates seemed to differ between PS and PE probably due to the differences in the molecular structure and tensile strength between the two polymers.

Based on the above, heterogeneous photocatalysis was successfully coupled with physical or chemical processes altering the degradation kinetics and/or overall efficiency to promote the global performance of the technology. For instance, when combining heterogeneous photocatalysis with biological treatment, membrane reactor, membrane photoreactor, or physical adsorption, the photocatalytic mechanisms are not affected but the efficiency of the overall process is improved. When heterogeneous photocatalysis is coupled with ultrasonic irradiation, ozonation, electrochemical treatment, or photo-Fenton reaction, the photocatalytic mechanisms are in this case modified, thus improving the efficiency of the process (Augugliaro et al., 2006). Therefore, various researchers have combined the Fenton reactions with photocatalysis to create a novel wastewater treatment approach. Utilizing this strategy, a win–win situation could be attained. This will not only extend the lifetime of produced charge carriers, yet it will also accelerate the Fe^{3+}/Fe^{2+} cycle, resulting in increased mineralization of pollutants and a reduction in iron sludge. As an example, **Figure 5** depicts a hypothesized CdS/CNT-TiO_2 process for photo-Fenton degradation of methylene blue when exposed to visible light. As seen, the photo-induced electron (e_{cb}^-) generated on TiO_2's surface can be scavenged by O_2, while the photo-induced hole (h_{vb}^+) reacts with OH^- or H_2O. In addition, the adsorbed Fe^{3+} on TiO_2's surface can be reduced by the transfer of electrons, accelerating the Fe^{3+}/Fe^{2+} cycle and impeding the electron–hole recombination. Lastly, the electron transfer between the excited state of the photosensitizer (MB*) and Fe^{3+} leads to the regeneration of Fe^{2+} ions and therefore increases the kinetic rate of the degradation process (Kim and Kan, 2015).

TABLE 1 | Main studies of MPs' photocatalysis.

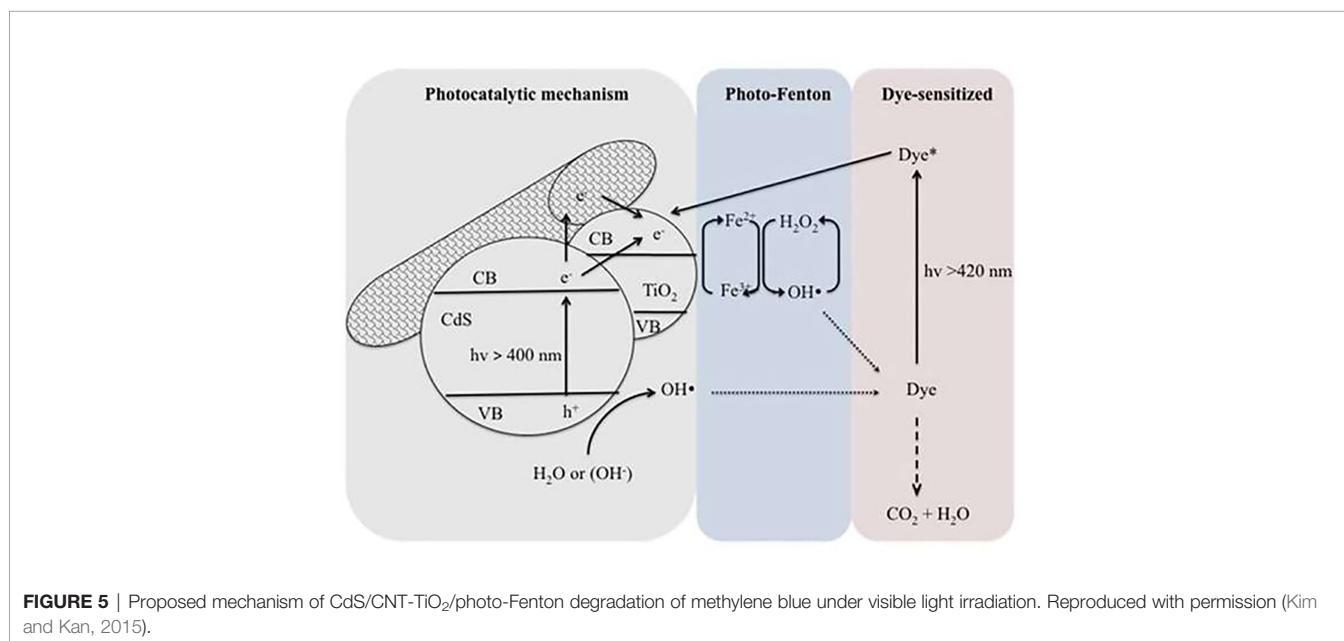| Photocatalysts	MPs type	MPs appearance	Light source	Irradiation time	Degradation system	Reaction conditions	MPs characteri-zation technique	Efficiency	References
TiO_2 powder	PVC	Powder	UV	300 h	Solid	PVC film size = 75 cm × 50 × 30 µm; 200 W mercury lamp (1.5 mW/cm^2); distance = 22 cm	UV-VIS, FTIR, GPC, XPS, SEM	27%	Cho et al. (2001) (Cho and Choi, 2001)
TiO_2; TiO_2/CuPc nanoparticles	PS	Appliance	Fluorescent light	250 h	Solid	PS appliance: 0.5 g; dropped on the catalyst films; 8 W fluorescent lamp (1.75 mW/cm^2); distance = 7 cm	Weight loss, UV-VIS, SEM	N/A	Shang et al. (2003) (Shang et al., 2003)
TiO_2 nanotube, TiO_2 nanoparticles	LDPE	Film	UV and visible light	15 days; 45 days	Solid	Initial LDPE film size = 3 cm × 3 cm; 18 W UV lamp of wavelength 315 nm (2.54 mW/cm^2); 5 W halogen (6.76 mW/cm^2); distance = 5 cm	XRD, EDS, UV-Vis, SEM, UTM, FTIR	CI = 1.2; CI = 1.39	Ali et al. (2016) (Ali et al., 2016)
ZnO nanorods	LDPE	Film	Visible light	175 h	Liquid	LDPE film of size (1 cm^2); 50 W dichroic halogen lamp (6–70 Klux); distance = 10 cm	SEM, optical microscope, FTIR, DMA	CI = 1.38	Tofa et al. (2019) (Tofa et al., 2019)
Pt-ZnO nanorods	LDPE	Film	Visible light	175 h	Liquid	LDPE film of size (1 cm^2); 50 W dichroic halogen lamp (6–70 Klux); distance = 10 cm	SEM, optical microscope, FTIR, DSC, TGA	CI = 1.6	Tofa et al. (2019) (Tofa et al., 2019)
ZnO nanorods	PP	Particle	Visible light	456 h	Liquid	Initial PP MP particles = ~ 70 mg, ~ 10^4 particles/L; 120 W tungsten halogen lamp (60 mW/cm^2); distance = 20 cm	SEM, optical microscope, FTIR, DSC, GC-MS, TGA	65%	Uheida et al. (2020) (Uheida et al., 2020)
BiOCl nanoflower and nanodisk	PS	Composite film	Visible light	90 h	Solid	Initial PS film size = 78 cm^2; 500 W halogen luminaire lamp; distance = 5 cm	XRD, UV-Vis, SEM, AFM, FTIR	N/A	Sarwan et al. (2020) (Sarwan et al., 2020)
PPy/TiO_2	PE	Composite	Sunlight	240 h	Liquid	Experiment carried out on a sunny day under ambient conditions from 10:00 a.m. to 4:00 p.m.	GPC, AFM, FT-IR, weight loss	54.4%	Li et al. (2020) (Li et al., 2020)
TiO_2 nanoparticles	PS	Microspheres	UV	12 h	Liquid	PS spheres: 400 nm; dropped on the catalyst films; UV lamp (<365 nm); distance = 10 cm	FE-SEM, Raman Spectroscopy, GC, HPPI-TOFMS	98.40%	Nabi et al. (2020) (Nabi et al., 2020)
	LDPE	Film	UV and visible light	36 h	Solid	UV lamp (<254 nm and <365 nm); distance = 10 cm	FE-SEM, Raman Spectroscopy, GC, HPPI-TOFMS	N/A	
TiO_2 powder	PA66	Microfiber	UVA	105 h	Liquid	PA66: 10 µm; 8 W UVA lamp (365 nm); distance = 5 cm	Weight loss, FTIR, COD, SEM	19%	Lee et al. (2020) (Lee et al., 2020)
	PA66	Microfiber	UVC	105 h	Liquid	PA66: 10 µm; 8 W UVC lamp (254 nm); distance = 5 cm	Weight loss, FTIR, COD, SEM	27%	
Protein-based porous N-TiO_2	HDPE	Scrubs	Visible light	20 h	Liquid	HDPE MPs = 60 g; 27 W fluorescent lamp (λ = 400)	ATR-FTIR, SEM, weight loss	6.40%	Ariza-Tarazona et al. (2020) (Ariza-Tarazona et al., 2019)
	HDPE	Scrubs	Visible light	8 h	Liquid	PS NPs = 30.9 ml; 27 W fluorescent lamp (λ = 400)	ATR-FTIR, SEM, weight loss	2.86%	
Mesoporous N-TiO_2 nanoparticles	LDPE	Film	Visible light	50 h	Liquid	0.4 wt/v% of MPs; 50 W visible lamp (400–800 nm); room temperature; stirring = 300 rpm; distance = 21.5 cm; pH = 3	Optical microscope, FTIR, mass loss	~1%	Llorente-García et al. (2020) (Llorente-García et al., 2020)
	HDPE	Bead	Visible light	50 h	Liquid	0.4 wt/v% of MPs; 50 W visible lamp (400–800 nm); room temperature; stirring = 300 rpm; distance = 21.5 cm; pH = 4	Optical microscope, FTIR, mass loss	4.65%	

(Continued)

TABLE 1 | Continued

Photocatalysts	MPs type	MPs appearance	Light source	Irradiation time	Degradation system	Reaction conditions	MPs characterization technique	Efficiency	References
C, N-TiO2 Powders	HDPE	Scrub	Visible light	50 h	Liquid	50 ml of a 0.4 wt./vol % HDPE MPs; 50 W visible LED lamp (57.2 ± 0.3 W/m^2); pH 3; distance = 25 cm	FEI E-SEM, EDS optical microscope, FTIR	71.77 ± 1.88%	Vital-Grappin et al. (2021) (Vital-Grappin et al., 2021)
TiO$_2$-nanotubular structure	PS	Nanoparticles	UV	50 h	Liquid	0.9% w/v of PS-NPs; UV lamp (0.021 mW/cm^2); distance = 10 cm	Turbidity, TOC, FTIR, GC-MS	19.70%	Domínguez-Jaimes et al. (2021)
TiO$_2$-barrier structure	PS	Nanoparticles	UV	50 h	Liquid	0.9% w/v of PS-NPs; UV lamp (0.021 mW/cm^2); distance = 10 cm	Turbidity, TOC, FTIR, GC-MS	15.00%	(Domínguez-Jaimes et al., 2021)
TiO$_2$-mixed structure	PS	Nanoparticles	UV	50 h	Liquid	0.9% w/v of PS-NPs; UV lamp (0.021 mW/cm^2); distance = 10 cm	Turbidity, TOC, FTIR, GC-MS	23.50%	
BiOCl	PE	Microspheres	UV	10 h	Liquid	1 g/L PE; 250 W Xe lamp (<420 nm)	FTIR, SEM	5.38%	Jiang et al. (2021) (Jiang et al., 2021)
NiAl$_2$O$_4$	LDPE	Film	Visible light	5 h	Liquid	Initial LDPE film size = 3 cm × 3 cm; 350 W halide lamp; distance = 25 cm	Weight loss, FTIR, XPS	12.50%	Venkataramana et al. (2021) (Venkataramana et al., 2021)
TiO$_2$/β-SiC alveolar foams	PMMA	Nanobeads	UV-A	7 h	Liquid	300 mg of commercial monodisperse solution; Philips T5 15 W 10 Actinic BL (112 mW/cm^2); fow rate = 10 ml/min; pH = 6.3; distance = 1 cm	TOC	50%	Allé et al. (2021) (Allé et al., 2021)

N/A, Not Applicable.

5 PHOTOCATALYTIC MECHANISM OF MICROPLASTICS DEGRADATION

The solid-state photocatalytic degradation of polymer started back in 1970, yet the investigations on the removal of MPs in an aqueous environment have recently started and the mechanism is not fully known (Padervand et al., 2020; Xu et al., 2021).

Light absorption, electron–hole separation, and the generation of highly ROS such as $O_2^-/\dot{O}H/HO_2^-$ are the three main stages in a photocatalysis process. These radicals start the degradation process within the polymeric chain when exposed to light and humidity. The fundamental photocatalytic degradation mechanism of plastic can be classified into four steps: initiation, propagation, branching, and termination (Rabek Jan, 2012).

FIGURE 5 | Proposed mechanism of CdS/CNT-TiO$_2$/photo-Fenton degradation of methylene blue under visible light irradiation. Reproduced with permission (Kim and Kan, 2015).

The initiation step is caused either by the abstraction of hydrogen or by the session of the C–C bond at the impure centers, generating alkyl radicals of MPs. The presence of photocatalyst increases the generation of alkyl radicals using active species. Peroxy-radicals and hydroperoxides are formed during chain propagation. Further oxidation stimulates chain branching and scission with the generation of low-molecular-weight oxygenated compounds like hydroxyl, peroxide, and carbonyl groups leading to micro-cracks within the polymeric surface (Cho and Choi, 2001; Shang et al., 2003; Zhao et al., 2007; Yousif and Haddad, 2013; Ali et al., 2016; Tofa et al., 2019; Miao et al., 2020). The general mechanism of photo-oxidative degradation reactions of MPs is shown in **Table 2** below, reproduced with permission from (Singh and Sharma, 2008; Tofa, 2018).

Tofa et al. (2019) (Tofa et al., 2019), Sarwan et al. (2020) (Sarwan et al., 2020), and Cho et al. (2001) (Cho and Choi, 2001) proposed photocatalytic degradation mechanisms of LDPE, PVC, and PS, respectively. LDPE film was exposed to visible light irradiation for 175 h using ZnO and Pt-ZnO as catalysts in the study of Tofa et al. (2019) (Tofa et al., 2019). They observed that alkoxy radicals are the key interim species that produced carboxylic groups like aldehydes, ester, ketones, and carboxylic acids in the photo-oxidation process and found ketone as the key species that undergoes further oxidation and results in complete mineralization, similar to solid-phase LDPE degradation using TiO_2 conducted by Ali et al. (2016) (Ali et al., 2016). The proposed degradation mechanism is adapted with permission from Tofa et al. (2019), and shown in **Figure S3A**.

The degradation mechanism in **Figure S3B** of solid-phase PVC was proposed by Cho et al. (2001) (Cho and Choi, 2001). Distinctive wrinkles and cavities occurred on the surface of PVC after 100 h of irradiation using TiO_2 under UV light. It was clear from the weight loss study that photocatalytic degradation was much faster than photolytic degradation. Miao et al. (2020) reported identical reactions when experimented on a liquid-phase condition of PVC (Miao et al., 2020).

Sarwan et al. (2020) conducted photocatalysis of PS film under visible light using Bismuth oxychloride (BiOCl) nanoflower and nanodisk for 90 h in a liquid phase and a mechanism in **Figure 6** was proposed (Sarwan et al., 2020). Similar research but in a solid phase was conducted by Shang et al. (2003) on PS plastic under the sunlight with the formation of a small number of by-products. The solid-phase photocatalytic oxidation of PS plastic film was conducted using TiO_2 and TiO_2/CuPc (copper phthalocyanine) powder for 250 h (Shang et al., 2003). They revealed that the degradation kinetics depended on the number of ROS generation.

As discussed above, the photocatalytic degradation of MPs either in the solid phase or in the liquid phase is in good agreement with the basic principles: initiation, chain propagation, branching cross-linking, and session.

6 CHARACTERIZATION TECHNIQUES OF MICROPLASTICS

Various characterization techniques are available for observing the degradability of MPs, which can be broadly classified into elemental, morphological, thermal, mechanical, and chemical analyses (Kumar et al., 2009). **Table 3** illustrates the most often accessible options and their applications.
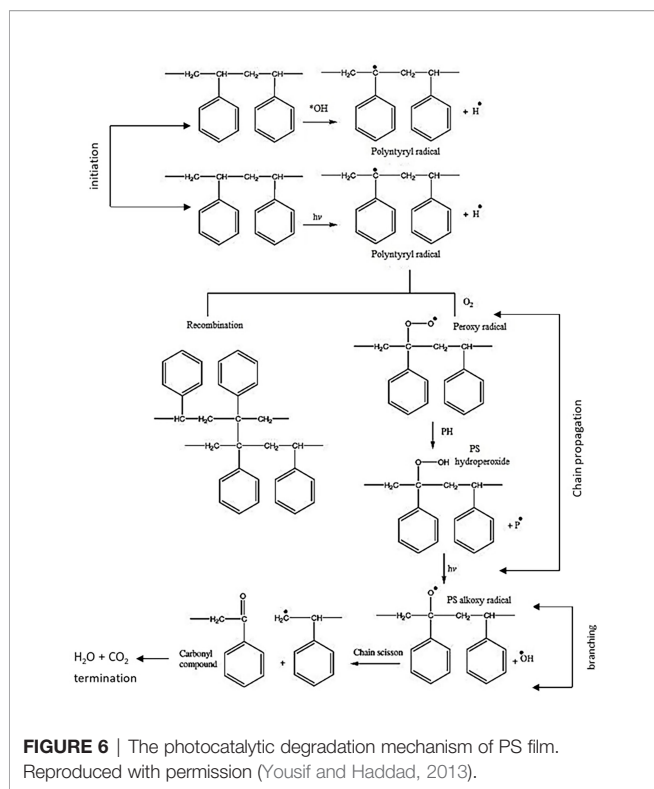
6.1 Elemental Composition
Elemental composition is an analytic tool for identifying the composition of copolymers, plastic blends, and molecular weight. Each plastic material has a characteristic molecular weight, chemical composition, and binding state that may alter after photocatalytic degradation.

Many studies have determined molecular weight through tools like gel permeation chromatography (GPC), nuclear magnetic resonance (NMR), viscosimetry, and osmometry, which have limited application to only soluble plastics. GPC, also known as size exclusion chromatography, is a fast, efficient, and most commonly used technique that measures a wide range of molecular weight and polydispersity index (De los Santos-Villarreal and Elizalde, 2013). Liang et al. (2013) conducted a high-temperature GPC analysis to determine the fluctuations in the molecular weight of the LDPE film before and after UV irradiation in which the temperature of the GPC injector, column, and the detector was kept at 150°C (Liang et al., 2013). 1,2,4-trichlorobenzene was employed in the mobile phase with an elution rate of 1.00 ml/min. The photo-

---

TABLE 2 | The general mechanism of photocatalytic degradation of MPs.

Steps	Reactions
Initiation	-H + energy (hν) → $^\bullet$ (polymer alkyl radical) + H$^+$
	-H + $^\bullet$OH → $^\bullet$ (polymer alkyl radical) + H$^+$
Chain Propagation	$^\bullet$ + O_2 → OO$^\bullet$ (polymer per-oxyradical)
	MPOO$^\bullet$ + PH → POOH (polymer hydroperoxide) + P$^\bullet$
Chain Branching	OOH → O$^\bullet$ (polymer alkoxy radical) + $^\bullet$OH
	2OOH → OO$^\bullet$ + O$^\bullet$ + H_2O
	O$^\bullet$ + H → OH + $^\bullet$
	H + $^\bullet$OH (hydroxyl radical) → $^\bullet$ + H_2O
Chain scission/Termination	2OO$^\bullet$ → inert products
	2 $^\bullet$ → MP-MP
	OO$^\bullet$ + $^\bullet$ → OO

$^\bullet$-H – Microplastic

FIGURE 6 | The photocatalytic degradation mechanism of PS film. Reproduced with permission (Yousif and Haddad, 2013).

irradiation of LDPE composites decreased the molecular weight to smaller values due to the production of low-molecular-weight compounds.

NMR spectroscopy is comparatively expensive but accurate, providing information (both qualitative and quantitative) on molecular structure, molecular weights, molecular weight distribution, chain orientation, and molecular motion of any unknown MP that is incomparable to other methods (De los Santos-Villarreal and Elizalde, 2013; Carraher, 2018). In a work carried out by Izunobi and Higginbotham et al. (2011), R-methoxy-ω-aminopolyethylene glycol and R-methoxy-polyethylene glycol-block-poly-ε-(benzyloxycarbonyl)-L-lysine were dissolved in N-deuterated dimethyl sulfoxide (DMSO-d6); the solution was observed on a spectrometer (499.8 MHz) at 60°C to obtain NMR spectra (Izunobi and Higginbotham, 2011). They mentioned the inability of determining weight-average molecular weight (M_w) unlike the GPC method; therefore, its potential in molecular weight determination is not appreciated.

In contrast, osmometry and viscosimetry are relatively cheaper, less efficient, and suitable for MPs having high- and low-molecular-weight determination, respectively (De los Santos-Villarreal and Elizalde, 2013; Carraher, 2018).

Tools like x-ray photoelectron spectroscopy (XPS) has a broad application in detecting relative composition, depth profiling, and chemical state from the surface of MPs. Such a system is expensive, requires high vacuum conditions, and provides only surface information. Yet, XPS provides straightforward and non-destructive surface characterization information of chemical bonding, and the total elemental

composition of any MP. Each element demonstrates characteristic peaks and relative abundance when exposed to x-rays (Andrade, 1985). Celasco et al. (2014) used XPS for measuring surface texture and copolymer thickness in polyethylene glycol (PEG) nanocapsules prepared by solvent displacement method (Celasco et al., 2014). Miao et al. (2020) analyzed the elemental composition of PVC MPs before and after electrocatalytic oxidation using high-resolution XPS (Miao et al., 2020). The PVC surface morphology transformed significantly as identified by the change in the number of C, O, and Cl atoms.

6.2 Surface Morphology

The photodegradation of MPs generally starts at the external bulk surface and gradually goes deep (Tofa et al., 2019). Therefore, it is of immense importance to investigate the surface condition to understand the effects of degradation on the mechanical and physical properties of MPs. There are numerous techniques and tools for a surface analysis whose usability depends on different purposes. Here, we discuss a few conventional optical techniques and their serviceability in characterizing synthetic plastic materials.

A simple optical microscope has been a common technique to study the surface topography of a bulk structure in a reflected light mode. Tofa et al. (2019) (Tofa et al., 2019), Llorente-García et al. (2020) (Llorente-García et al., 2020), Uheida et al. (2020) (Uheida et al., 2020), and Vital-Grappin et al. (2021) (Vital-Grappin et al., 2021) used optical microscopes to observe the surface texture after the exposure. An optical microscope has underlying limitations of high magnification and restricted sample thickness between 5 and 40 mm. Digital imaging with scanning electron microscopy (SEM), transmission electron microscopy (TEM), and scanning probe microscopies are often used for image analysis and image processing (Galloway et al., 2002; Bonnet, 2004).

SEM offers both higher focus and larger depth of field and is a widely applicable technique for determining surface morphology, texture, and composition. A focused beam containing electrons is exerted to reach nano-scale imaging. MPs' surfaces must be coated with conductive materials to obtain any acceptable image (Carraher, 2018). SEM has been used to determine wrinkles, cracks, and cavities of varying sizes on commercial grade LDPE films as a result of photo-oxidation (Tofa et al., 2019). Liang et al. (2013) used SEM to display surface morphology and the chalking phenomenon of LDPE composite films after UV irradiation for 230 h (Liang et al., 2013). The image analysis found 1- to 2-μm-wide and 0.5- to 1-mm-deep cavities all over the LDPE/TiO_2 and LDPE/MPS-TiO_2 film surfaces.

Another useful, versatile, and high-resolution microscopy technique for different imaging competencies is TEM. It enables observing detailed structural information at an atomic level; magnifications may reach up to one million under good conditions. Images are usually detailed, offer bright field and dark field, and can capture chemical information of the sample. The imaging and the analytical capabilities improve when coupled with a spectrometer (Burge et al., 1982; Bonnet, 2004;

TABLE 3 | General techniques for characterization of MPs.

Categories	Technique	Application	References
Elemental composition	Gel permeation chromatography, GPC Nuclear magnetic resonance, NMR Viscometry Osmometry	Elemental analysis: molecular weight, chemical composition, binding states	Izunobi et al. (2011) (Izunobi and Higginbotham, 2011), De los Santos-Villarreal et al. (2013) (De los Santos-Villarreal and Elizalde, 2013), Liang et al. (2013) (Liang et al., 2013), and Carraher et al. (2013) (Carraher, 2018)
	X-ray photoelectron Spectroscopy, XPS	Surface profiling	Gelasco et al. (2014) (Celasco et al., 2014)
Morphological properties	Optical microscopy, OM	Surface texture; restricted thickness (5–40 mm); low cost	Tofa et al. (2019) (Tofa et al., 2019) and Liang et al. (2013) (Liang et al., 2013)
	Scanning electron microscopy, SEM	Vacuum technique; morphology, image analysis	
	Transmission electron microscopy, TEM	Detailed imaging and analysis; chemical information; interface	Motaung et al. (2012) (Motaung et al., 2012)
	Profilometer	nondestructive; rapid; determining surface irregularities, fractures, and roughness	Ali et al.(2016) (Ali et al., 2016)
Thermal properties	Differential scanning calorimetry, DSC	Kinetics and phase transitions; oxidative stability	Gregory et al. (1998) (Gregory, 1998) and Gill et al. (2010) (Gill et al., 2010)
	Thermogravimetry analysis, TGA	Polymer type; composition; weight loss; kinetic parameters	Zhao et al. (2007) (Zhao et al., 2007), Liang et al. (2013) (Liang et al., 2013), Celasco et al. (2014) (Celasco et al., 2014), and Uheida et al. (2021) (Uheida et al., 2020)
Mechanical properties	Universal testing machine, UTM	Determination of tensile strength; % elongation, elastic modulus; destructive method	Zhao et al. (2007) (Zhao et al., 2007), Liang et al. (2013) (Liang et al., 2013), and Ali et al.(2016) (Ali et al., 2016)
	Dynamic mechanical analyzer, DMA Lorentz contact resonance, LCR	Determination of viscous and elastic modulus; destructive method	Menard et al. (2020) (Menard and Menard, 2020), and Lup et al. (2021) (Luo et al., 2021)
Degradation kinetics	Mass balance	Simple; low-cost technique; degradation kinetics	Liang et al. (2013) (Liang et al., 2013), and Ariza-Tarazona et al. (2019) (Ariza-Tarazona et al., 2019)
	Turbidimetry	Monitoring of nanoplastics in an aqueous environment	Ma et al. (2019) (Ma et al., 2019), and Domínguez-Jaimes et al. (2021) (Domínguez-Jaimes et al., 2021)
	Chemical oxygen demand, COD	Cheap; degree of mineralization; degradation kinetics	Rajamanickam et al. (2016) (Rajamanickam and Shanthi, 2016)
	Total organic carbon, TOC	Low cost; concentration of total organic compounds; reaction kinetics	Giroto et al. (2010) (Giroto et al., 2010) and Allé et al. (2021) (Allé et al., 2021)
Degraded products	Gas chromatography, GC	Separates and analyzes volatile organic compounds of high molecular weight.	Hakkarainen et al. (2006) (Hakkarainen and Karlsson, 2006)
	Gas chromatography-mass spectrometry, GC-MS	Separate, quantify, and identify unknown species; qualitative and quantitative evaluations	Medeiros et al. (2018) (Medeiros, 2018)
	Liquid chromatography-mass spectrometry, LC-MS	Separate, quantify, and identify a wide range of species; molecular weight; end group analysis	Perez et al. (2016) (Perez et al., 2016)
	Fourier transformation infrared, FTIR spectroscopy	Non-destructive; cheap; identification and detection of structural transformation; determine the degree of oxidation	Ali et al. (2016) (Ali et al., 2016) and Almond et al. (2020) (Almond et al., 2020)

Carraher, 2018). In a study by Motaung et al. (2012), TEM was used for imaging the TiO_2-polymethylmethacrylate (TiO_2-PMMA) nanocomposites (Motaung et al., 2012).

6.3 Thermal Properties

Common instrumentation for monitoring thermal properties includes thermo-gravimetric analysis (TGA) and differential scanning calorimetry (DSC). DSC is a commonly used thermal analysis that is applied to determine the melting point, heat of fusion, crystallinity percentage, crystallization kinetics, phase transitions, and oxidative stability. The heat absorbed or radiated by any MP as a function of temperature against time is measured with DSC (Gill et al., 2010). The thermal analysis provides phase transition information, e.g., melting and glass-to-rubber transition to the crystalline and amorphous phases, respectively (Aguilar-Vega, 2013). Uheida et al. (2020) carried

out DSC measurements on visible light-exposed PP MPs irradiated at different lengths to investigate the change in the crystallization behavior (Uheida et al., 2020). They observed a shift in the melting point to lower temperatures due to the degradation of the polymeric chain.

While DSC measures the heat quantity, TGA measures the rate of change of weight as a function of temperature in a controlled environment. It has a wide application in determining the thermal and oxidative stabilities, and in the identification and composition of plastic material. Many studies have used TGA to confirm the change in the thermal properties and determined kinetic parameters after photocatalytic degradation of MPs by monitoring the weight loss (Liang et al., 2013; Uheida et al., 2020; Zhao and Zhang, 2021).

6.4 Mechanical Properties

Tensile tests are used to determine nominal tensile strength, elongation, and elastic modulus (Aguilar-Vega, 2013). Usually, tensile testing, a destructive method, is conducted following ASTM 882-85, the universal testing machine (UTM). Analysis of several studies shows that photocatalytic degradation has an adverse effect on the tensile strength of films. The samples become brittle and fragile. Also, percent elongation decreases as carbonyl group formation increases (Zhao et al., 2007; Liang et al., 2013; Ali et al., 2016).

A dynamic mechanical analyzer (DMA) is extensively used for measuring viscoelastic properties of MPs at a molecular level where a minor deformation is applied to a given sample. This permits the materials to undergo cyclic loading, which causes both elastic and viscous deformation. The amorphous and crystalline parts of the material cause elastic component deformation, while the viscous part is induced by the movement of polymer segments (Menard and Menard, 2020). In the work of Tofa et al. (2019) photo-irradiated LDPE films were exposed to a DMA that resulted in the strain as a function of temperature at a frequency of 1 Hz (Tofa et al., 2019). The result elucidated the loss of elasticity after photocatalytic activities due to chain scission of LDPE films.

Recently, Luo et al. (2021) used a Lorentz contact resonance (LCR) technique for determining the viscoelastic properties of nanoscale TiO_2-coated MPs by measuring the contact stiffness between the AFM probes and MPs (Luo et al., 2021). It provides a high-resolution map of different phases on extremely thin films. A greater frequency was associated with a stiffer MPs material, while a lower frequency was associated with a smoother material. The MPs became stiffer with increasing irradiation, forming wrinkles, cracks, and fragmentation.

6.5 Kinetic Degradation of Microplastics

The determination of kinetics is of immense importance to understanding the degradation mechanism and predicting the stability and life span. Here, we discuss a few simple techniques for determining the degradation kinetics of MPs.

The utilization of weighing balance is a simple, low-cost technique to study weight loss during photocatalytic degradation (Liang et al., 2013; Ali et al., 2016; Ariza-Tarazona et al., 2019). For Lee et al. (2020), weight loss was determined to

evaluate the photocatalytic degradation kinetics of the PA66 microfibers using different doses of TiO_2 and by changing UV wavelength (Lee et al., 2020). It was elucidated that the shorter UV wavelengths were more efficient in damaging PA66 microfibers in comparison with the longer ones. They discovered that the initial kinetic rate is precisely proportional to the catalyst dose.

Turbidity is a measure of the degree of losing transparency due to the presence of suspended particulates in the water. A turbidimeter, a cheap, widely used tool for monitoring drinking water quality, measures this haziness in water (Gregory, 1998). Ma et al. (2019) used a turbidimeter to observe the elimination of PE using coagulant $AlCl_3.6H_2O$ and $FeCl_3.6H_2O$ at different doses. Under low pH, a 5 mM dose $AlCl_3.6H_2O$ ensured higher removal efficiency of PE particles (Ma et al., 2019). A pseudo-first-order kinetics of PS after in an aqueous environment was calculated using turbidity data (Domínguez-Jaimes et al., 2021).

Chemical oxygen demand (COD) in addition to total organic carbon (TOC) could be employed to evaluate the mineralization of MPs. COD is a measure of the requirement of oxygen for the oxidation of both organic and inorganic matters present in water, by a strong chemical oxidant. COD can evaluate the degree of mineralization that had generated during the photocatalytic process of MPs (Rajamanickam and Shanthi, 2016; Lee et al., 2020). On the other side, TOC has been in practice for exploring the concentration of total organic compounds (TOCs) in aqueous solution before and after photooxidative degradation (Giroto et al., 2010). For instance, polymethylmethacrylate and PS nanobead solutions were degraded using UV irradiation of $TiO_2/\beta–SiC$ alveolar foams, wherein reaction kinetics and TOC value were found to increase with the shorter wavelength. The TOC value ensures the breakdown of PS MP in suspension (Allé et al., 2021). Another research group used a TOC analyzer to investigate the degree of mineralization of PVC as a function of temperature using an electro-Fenton technology. Under the electrocatalysis process combined with high temperature (100°C), TOC can greatly increase. They also suggested that TOC values can be relied on reflecting the decomposition of PVC MPs (Miao et al., 2020).

6.6 Characterization Techniques for Produced By-Products

GC, GC-MS, and FTIR are the most commonly used tools for assessing MP degradation and by-products. The chromatograph is a destructive technique. In contrast, FTIR is a non-invasive method to identify and characterize transformation in chemical structure.

GC is the most popular analytical tool for monitoring by-products after degradation. GC is not suitable for the analysis of organic compounds having high molecular weight or low vaporization temperatures (Hakkarainen and Karlsson, 2006). Zhao et al. (2007) utilized GC to determine the concentration of CO_2 and volatile organics generated during photocatalytic degradation of PE under solar and UV light. They proposed that CO_2 is the key element produced from the photocatalytic degradation of PE plastic (Zhao et al., 2007). Other volatile organics like methane, ethene, ethane, propane, acetaldehyde,

formaldehyde, and acetone were also detected, albeit of a lesser amount. GC was also used to study the photocatalytic degradation of PS plastic exposed to fluorescent light, and generation of volatile organic compounds followed by CO_2 evolution was confirmed (Shang et al., 2003).

Polymer degradation constituents have been investigated by many scientists using GC-MS (Barlow et al., 1961). It permits both qualitative and quantitative evaluations (Medeiros, 2018). GC-MS analyzed obtained by-products from photocatalytic degradation of PP MPs over ZnO nanorods. It has been found that ethynyloxy/acetyl radicals, hydroxypropyl, butyraldehyde, acetone, propenal, and the pentyl group are the most abundant degraded by-products (Uheida et al., 2020). During the investigation of degraded species after oxidation of PVC MPs *via* an electro-Fenton system, short-chained organics like alkenes, alcohols, monocarboxylic acids, dicarboxylic acids, and esters were detected (Miao et al., 2020).

LC-MS is a highly sensitive tool, mostly suitable for MP identification, sensing lower volatile compounds of high polarity, determining molecular weight, and conducting end group analysis of polymers. Sample preparation is comparatively easy, and it has the ability to recognize and measure a wider range of compounds (Perez et al., 2016). Tapia et al. (2019) recently used LC-MS and developed a method for identifying the degradation compounds of a cross-linked polyester for biomedical relevance (Tapia et al., 2019). They used both LC-MS and LC-MS/MS for characterizing structural isomers and their corresponding structures.

ATR-FTIR spectroscopy is a widely used non-destructive technology for measuring infrared spectra for a variety of materials, especially for indicating the structural transformation in MP structure after degradation. This is an inexpensive, sensitive, and time-saving analytical method that provides an indirect result of the extent of oxidation of polymeric materials. The functional group within polymeric compounds vibrates at its own characteristic frequency due to the absorption of IR light. FTIR spectroscopy is applicable for the identification and detection of structural transformation in plastic materials (Tofa et al., 2019; Almond et al., 2020). Numerous studies on chemical transformation within polymeric chains using FTIR have been reported (Cho and Choi, 2001; Shang et al., 2003; Tofa et al., 2019).

7 SCALING-UP OF THE PHOTOCATALYTIC REACTORS

While the coupling of AOP technologies is very beneficial to increasing the photocatalytic activity of the process, the performance of photoreactors remains dependent on several factors such as (i) the operational mode; (ii) the several phases that exist in the reactor; (iii) the hydrodynamics; and (iv) the reacting mixture's composition and operating conditions. Because photocatalytic oxidation reactions are caused by absorbed photons with adequate energy values by the SC particles, the photoreactor and radiation sources are the most important components of a photocatalytic/Fenton process (Sacco et al., 2020).

Dedicated photocatalytic reactors for water treatment can fall into two categories: (1) reactors with photocatalyst deployed as suspended particles requiring a supplementary downstream separation unit for photocatalyst recovery, and (2) reactors with a supported photocatalyst, which allows continuous operation (Pozzo et al., 2000; Chong et al., 2010). Although both configurations can be used to treat wastewater streams, when designing field-scale photoreactors, several parameters must be considered, including pollutant concentration (COD initial load), flow type and rates, light intensity, solar irradiation area, dissolved oxygen concentration in water in a state of equilibrium with the atmospheric air (Gutierrez-Mata et al., 2017), and the electrical energy per order EE/O (given in kWh in European countries) necessary to eliminate a contaminant by one order of magnitude (90%) in 1 m^3 of polluted water (Bolton et al., 2001; Vaiano et al., 2019). The composition and concentration of real wastewater effluents, as well as fluctuations in the photonic solar flux throughout the degradation process, make field-scale reactors a highly difficult challenge (Gutierrez-Mata et al., 2017). Due to the difficulties in controlling all the parameters cited above, for the scale-up of a photoreactor, often mathematical models are prepared including several sub-models (Cassano et al., 1995; Fagan et al., 2016) such as the radiation emission model, the radiation absorption-scattering model, the kinetic model, and the fluid-dynamic model (Cassano and Alfano, 2000). Such interconnected sub-models produce a complicated scheme of integral–differential equations that necessitate numerical solutions (Alvarado-Rolon et al., 2018). The local volumetric rate energy absorption (LVREA), which is termed as the energy attributable to the absorbed photons/(time and volume) inside the photoreactor, is a function of the photocatalytic reaction rate. This energy (LVREA) is highly reliant on the analytical solution of the radiation transfer equation (RTE), which is linked to the categories of lights and reactor geometry (Satuf et al., 2007).

Numerical computing approaches such as the statistical Monte Carlo method (MC) or analytical simplified methods such as the two-flux model (TFM) and the six-flux model (SFM) can also be used (Kim and Kan, 2015). MC, however, needs large computational processors, and TFM and SFM are limited to flat slab geometries (Li Puma, 2005; Moreira et al., 2010). CFD models were developed for scaling-up of dedicated photoreactors for wastewater treatment taking into account model pollutants, such as oxalic acid (Denny et al., 2009), phenol (Jamali et al., 2013), poly (vinyl alcohol) (Ghafoori et al., 2014), tributyl phosphate (TBP), tri (2-chloroethyl) phosphate (TCEP) (Moghaddami and Raisee, 2012), rhodamine B (Kumar and Bansal, 2013), methylene blue (Vaiano et al., 2015a), and emerging contaminants such as atrazine (Bagheri and Mohseni, 2015).

8 SELECTION OF REACTOR DESIGN FOR UP-SCALING

Before deciding to scale up a photoreactor, the performance of each configuration should be first established. As a result,

photoreactor energy efficiency is measured by the quantum yield, which is the ratio of reaction rate over the light absorption rate (Kim and Kan, 2015). The quantum yield is then transformed into a photochemical thermodynamic efficiency factor, which is denoted by (Serrano and De Lasa, 1997):

$$\eta = \frac{Q_{used}}{Q_{absorbed}} = \frac{r_{OH} \times \Delta H_{OH} \times W}{Q_{absorbed}} \tag{1}$$

Where r_{OH} is the rate of OH radical formation (mol/g of catalyst), ΔH_{OH} is the enthalpy of OH radical formation (J/mol), and W is the mass of catalyst (g). The energy efficiency factors cannot be employed for the specified reactor performance comparison because the treated volume and reactor footprint parameters are not integrated into the above equation (Gaya and Abdullah, 2008). Consequently, figures of merit in terms of collector area per mass (A_{CM}), which is the required collector area required to degrade 1 kg of pollutant in 1 h following a solar radiation of 1000 W/m^2 intensity, and collector area per order (A_{CO}), which is the required collector area to reduce the pollutant concentration in 1 m^3 by one order of magnitude (Bolton et al., 2001), were suggested for comparison of advanced oxidation technology (AOT) reactors of various configurations, as shown in the following equation (Bandala and Estrada, 2007; Rao et al., 2012):

$$A_{CM} = \frac{A_r \times \bar{E}_s \times t \times 1000}{M \times V_t \times E_s^0 \times t_0 \left(C_i - C_f\right)} \tag{2}$$

$$A_{CO} = \frac{A_r \times \bar{E}_s \times t}{V_t \times E_s^0 \times t_0 \times log \frac{C_i}{C_f}} \tag{3}$$

where A_{CM} and A_{CO} are in m^2/kg and m^2/m^3 order, respectively, A_r is the actual reactor area (m^2), t and t_0 are irradiance and reference time (h), $\bar{E}_s$ and E_s^0 are the average solar irradiance and reference solar irradiance (W/m^2), V_t is the treated volume (L), M is the molar mass (g/mol), and C_i and C_f are the initial and final pollutant molar concentrations, respectively. Therefore, the geometry of photocatalytic reactors would be preferably selected in such a way that the emitted irradiations are collected in maximum values.

9 PHOTOCATALYTIC REACTOR: CONFIGURATION AND COMMERCIALIZATION

Photochemical systems in addition to reactors have adopted conventional solar thermal collector designs, including parabolic troughs and non-concentrating collectors because the required hardware for solar photocatalysis is quite comparable to that required for thermal applications (Goswami, 1997). However, it should be noted that contrary to solar thermal processes, solar photochemical processes utilize solely high energy with short-wavelength photons. For instance, a TiO$_2$ photocatalyst operates under UV or near-UV sunlight (300 to 400 nm), and a photo-Fenton heterogeneous photocatalyst operates within sunlight wavelength radiation below 580 nm.

The prime benefits and shortcomings of concentrating and non-concentrating collectors for solar photocatalytic applications are as listed in **Table 4** (Malato et al., 2007).

Quantitative comparisons of photoreactor designs are quite challenging due to the broad diversity of photoreactor designs, operating conditions, photocatalyst design and preparation, changes in solar intensity, and kinds of pollutants. As a result, the comparisons are primarily qualitative and centered on the practical aspects of each design (Braham and Harris, 2009).

9.1 Parabolic Trough Reactors

A parabolic trough reactor (PTR) focuses solar energy on a transparent tube located along the parabolic focal line and whereby the reactant fluid flows using a long, reflective parabolic surface (see **Figure 7**). Concentration factors of 5 to 30 suns are commonly utilized for photocatalytic applications, while a concentration factor of 70 suns has been observed utilizing a parabolic dish reflector (Alfano et al., 2000; Malato et al., 2002; Oyama et al., 2004).

Increasing the intensity of the incoming light allows the use of a reduced quantity of photocatalyst leading to a reduction of the operating costs, as well as simplified catalyst separation and recycling (Goswami et al., 2004). This also enables the use of a smaller diameter absorber tube, allowing for higher operational pressures, which is beneficial in industrial-scale plants where

TABLE 4 | Comparisons between parabolic and non-concentrating solar photoreactors.

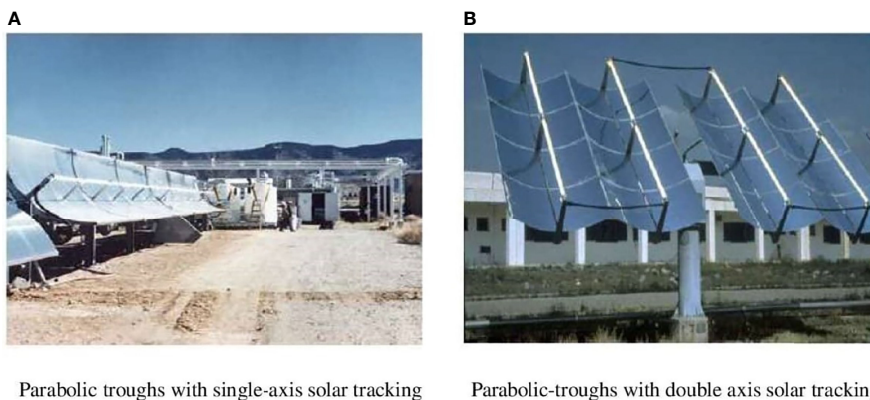|	Advantages	Disadvantages
Concentrating collectors	- Turbulent flow - Compounds free vaporization - More practical usage of supported catalysts - Smaller reactor tube area	- Direct radiation solely in addition to water overheating - High cost due to sun tracking system - Low optical efficiency - Low quantum efficiency (r = k I <1 with TiO$_2$)
Non concentrating reactors	- Diffused and direct radiation - No heating - Cost effective - High optical efficiency - High quantum efficiency (r = k I with TiO$_2$)	- Laminar flow with low mass transfer - Vaporization of reactants - Contamination of reactants - Weather resistance, chemical inertness, and UV transmission

A Parabolic troughs with single-axis solar tracking

B Parabolic-troughs with double axis solar tracking

FIGURE 7 | Parabolic troughs reactor types with **(A)** single and **(B)** double axis solar tracking. Reproduced with permission (Malato et al., 2007).

hundreds of meters of absorber tubing and associated components can result in considerable pressure losses (Alfano et al., 2000).

PTR configuration was applied in Sandia National Laboratory, New Mexico (SNL) for the treatment of 1,100 L of polluted water by salicylic acid using TiO$_2$ slurry. The employed PTR was 218 m long and 2.1 m wide, with a 38-mm-diameter borosilicate glass pipe. With a total aperture size of 465 m^2 and a concentrating ratio of 50, the device was able to achieve 96% degradation in just 40 min. The same system was used for treating other molecules such as trichloroethylene, tetrachloroethylene, chloroform, trichloroethane, carbon tetrachloride, and methylene chloride (Prairie et al., 1991). CIEMAT71, a Spanish corporation, and an American partnership consisting of the National Renewable Energy Laboratory (NREL), Lawrence Livermore National Laboratory (LLNL), and Sandia National Laboratories (SNL) built similar systems (Mehos et al., 1992). The CIEMAT development consisted of 12 "Helioman" units that were placed in sequence at the Plataforma Solar de Almeria (PSA) in Spain. Four parabolic trough aluminized reflectors with an overall collection area of 29.2 m^2 and two-axis tracking constituted each Helioman. The concentration factor of this configuration is approximately 6 suns, and the photonic efficiency (expressed as moles of degraded contaminant per incident mole of photons inside the reactor) was registered as ~1% (Malato et al., 2002). This PTR configuration turned out to be efficient for the photocatalytic degradation of pentachlorophenol (Minero et al., 1993), oxalic acid (Bandala et al., 2004), and 2,4-chlorophenol (Malato et al., 1997) contaminants in water. In addition, for the treatment of trichloroethylene by a suspended photocatalyst supplied at 0.8 g/L, the NREL consortium used single-axis tracking PTRs stacked in series over two drive trains with a collection area of 78 m^2 each and a concentration factor of ~20 suns (Mehos et al., 1992). A significant decrease in trichloroethylene concentration in contaminated groundwater beneath the level considered drinkable (from 106 ppb to <0.5 ppb) was observed in this installation.

However, there are various drawbacks associated with the use of PTR reactors. PTR can only collect and benefit from direct sunlight, which reduces the overall quantity of collectible solar radiation and makes the use of a solar tracking system inevitable, making their use quite expensive and inefficient on cloudy days. Overheating of the reaction solution is another key flaw of PTR (Blanco-Galvez et al., 2007). While heating the reaction fluid is normally good for enhancing the reaction rate (Falconer and Magrini-Bair, 1998), it may become unpleasant at higher concentration factors because of the possible formation of unwanted products through direct photolysis. Overheating can also lead to leaks and corrosion (Adesina, 2004), and can affect treatment efficiency. Moreover, an increase in the temperature leads to a decrease in the solubility of oxygen in the water and therefore bubble generation. Because O$_2$ is required for reaction completion (Prairie et al., 1991), the endless contribution of oxygen to the reaction or addition of scavengers such as hydrogen peroxide/sodium persulfate becomes essential for the process (Minero et al., 1993), which will complicate the water purification procedure and deteriorate its practicality. Because of the elevated operation cost related to water cooling, the existence of moving parts, and solar tracking devices, PTRs are not generally considered for scaling-up and commercialization.

Finally, the National Solar Thermal Test Facility at Sandia Laboratories in Albuquerque, New Mexico (USA) constructed the first outdoor engineering-scale reactor in 1989 (**Figure 7**, left), and the PSA in 1990 designed and built the very first PTC engineering scaled-up solar photochemical facility designated for the detoxification of water in Europe (**Figure 7**, right) (Minero et al., 1993; Malato et al., 2007).

9.2 Compound Parabolic Concentrator

The reflector geometry in CPC grants reflection of indirect light onto the absorber tube surface leading to an increase in the total quantity of photons and allowing the photoreactor to operate on overcast days when direct beams are unavailable (Bockelmann et al., 1995). As a result, by employing a CPC setup, many of the issues related to PTR could be avoided. Therefore, according to the following equation, the concentration factor and the acceptance angle of a CPC are directly associated:

$$C_{CPC} = \frac{1}{\sin\theta_a} = \frac{a}{2\pi r} \qquad (4)$$

where C_{CPC} is the concentration factor, θ_a is the acceptance half-angle, α is the width of the reflector aperture, and r is the radius of the absorber tube. As a result, a CPC with a concentration factor equal to 1 sun (no concentration) will possess an acceptance half-angle equal to ~90°C, which means that all received light beams by the aperture (direct and diffuse) would be reflected in the absorber tube. The enhancement in the CPC performance over that of the PTRs was shown to range between 30% and 200% (Parra et al., 2001; McLoughlin et al., 2004a) owing to the ability of CPCs to harvest diffused beams and to usethem more efficiently (as a consequence of homogeneously illuminating the absorber tube) (McLoughlin et al., 2004b; Malato et al., 2007). Likewise, no sun tracking technology is required, decreasing the system's complexity and cost dramatically.

However, CPC reactors use a greater quantity of catalyst and wide absorber tubes compared to PTRs, making it necessary to work at low operating pressures (Fernández et al., 2005; Tanveer and Tezcanli Guyer, 2013). A schematic illustration and photo of a compound parabolic collector (CPC) are shown in **Figure 8** (Fendrich et al., 2018).

The CPC design was employed in several pilot-scale assemblies. The PSA in Spain built a modular array of six CPC modules for the degradation of dichlorophenol solutions with a maximum concentration of 200 mg/L. Not more than 100 min was enough to remove the pollutant when using an overall collection area equal to 8.9 m (2216). Such CPC configurations were effectively employed for the degradation of a wide spectrum of water contaminants, such as bacteria (Fernández et al., 2005) pharmaceuticals (Augugliaro et al., 2005), municipal wastewater (Kositzi et al., 2004), pesticides (Oller et al., 2006), and other resistant compounds (Sarria et al., 2004).

A non-concentrating CPC design using suspended photocatalytic technology was also developed in the European "Solardetox" project for the treatment of commercial wastewater by building a modular system having each module made up of 16 parallel, 1.5-m tubes backed by CPC reflectors (Blanco et al., 1999; Malato et al., 2002). A full-size demo plant was built in

HIDROCEN, Madrid (Blanco-Galvez et al., 2007). In a recirculating batch mode, the facility is completely automated and capable of treating 1,000 L of persistent non-biodegradable chlorinated industrial water pollutants. The plant has an overall aperture area of 100 m² and is made up of two rows of 21 CPC collectors connected in series (each one is 1.5 m × 1.5 m and contains 16 parallel glass tubes with an inner diameter of 29.2 mm) (Blanco et al., 1999). Similar collectors were utilized for treating paper mill effluents in Brazil and Germany (Machado et al., 2003; Sattler et al., 2004; Eduardo da Hora Machado et al., 2004) and paper mill effluents (Amat et al., 2005), surfactants (Amat et al., 2004), and textile dyes (Prieto et al., 2005) in Spain.

A new CPC-based plant was constructed in 2004 to treat pesticides remaining in water after the recycling of plastics. Recycling of plastic containers was followed by industrial cleansing of the shredded plastic, resulting in water polluted with very harmful persistent chemicals (pesticides). In a batch process, this photo-Fenton-based treatment was able to mineralize up to 80% of the TOC in the washing water (Fallmann et al., 1999; Sagawe et al., 2001; Rossetti et al., 2004). Photocatalysis mineralizes approximately 95% of the pollutants, while the activated carbon filter eliminates the remaining 5%. The plant includes four parallel rows consisting of 14 photocatalytic reactor modules built with 20 tubes/module, 2.7 m²/module, and installed on a 37°C inclined platform, based on CPC solar collectors (local latitude). The overall collector surface area is 150 m², and the combined volume of the photoreactor is 1,061 L (Blanco-Galvez et al., 2007).

In 2006, a new initiative was taken by effectively treating saline industrial wastewater with approximately 0.6 g/L of non-biodegradable α-methylphenylglycine (MPG) and 0.4–0.6 g/L TOC utilizing a combination of solar photo-Fenton and aerobic biological processes. It was made up of a solar CPCs photo-Fenton reactor (100 m²) and an aerobic biological treatment plant with a 1-m³ capacity fixed biomass activated sludge reactor. The combined system reached approximately 95% mineralization, wherein the photo-Fenton pre-treatment degraded 50% of the initial TOC, and the aerobic biological treatment eliminated 45% (Malato et al., 2007).
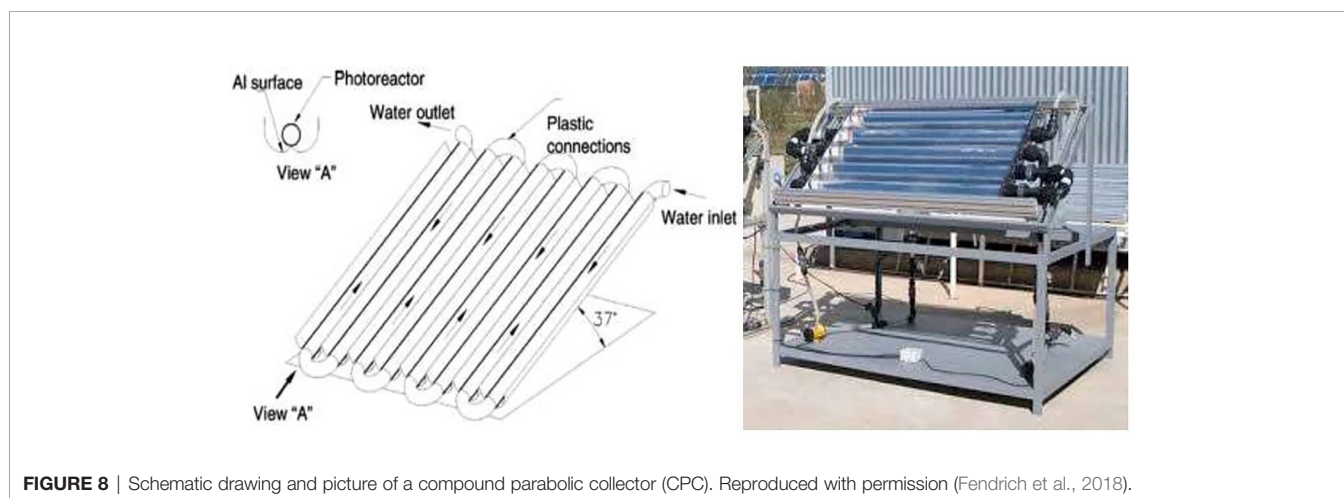

FIGURE 8 | Schematic drawing and picture of a compound parabolic collector (CPC). Reproduced with permission (Fendrich et al., 2018).

Zapata et al. (2010) established an approach for the development of a large-scale combination of solar photo-Fenton and aerobic biological systems for the remediation of commercially available pesticides using CPC reactors (Zapata et al., 2010). The industrial plant was made of a scaled-up biological treatment plant mainly consisting of two 1,230-L IBRs, a total collector with a 150-m^2 surface, and an overall photoreactor volume of 1,060 L. The combined industrial-scale system (photo-Fenton/bio) has an efficiency of 84%, with 35% belonging to the photo-Fenton treatment and 49% related to the biological process.

Solwater is an alternative project that disinfected bacterially contaminated water using CPC photoreactor technology with a supported photocatalyst and photosensitive dyes. This project is funded by the European Union and conducted in South America. Following 3 months of deployment, the removal efficiency was diminished due to the deposition of calcium carbonate over the photocatalyst and the photosensitizer (Navntoft et al., 2007). This decrease in TiO$_2$ efficiency was similarly observed when CPC packed with supported TiO$_2$ on glass beads was employed for remediating of resulting BTEX spiked molecules from secondary wastewater treatment (Miranda-García et al., 2001). Extending the efficiency of the reactor was achieved by using a filter of ~0.35 μm, and an anionic and cationic ion-exchange resin as a pretreating stage. Catalyst fouling problem was also seen in tubular type reactors packed with supported TiO$_2$ on silica spheres for urban wastewater treatment. Following a single month of treatment, iron sludge fouled the catalyst and dramatically reduced its efficiency (Nakano et al., 2004).

A CPC pilot-scale packed bed reactor made up of 5 Pyrex tubes (1.9 m length and 22.2 mm outer diameter) joined successively was employed for handling 21 L of triclosan solution over supported TiO$_2$ on volcanic mesoporous stones (Martínez et al., 2014). Finally, Silva et al. propose and tested a new approach for the remediation of landfill leachates following an aerobic treatment on a pilot scale (Silva et al., 2017). This approach consists of an aerobic activated sludge biological pre-oxidation (ASBO), coagulation, and sedimentation steps, and photo-oxidation through a CPC (10 modules, 20.8 m^2) photo-Fenton (PF) reactor. The optimal option for treating 100 m^3/day of leachate with a COD value less than 150 ppm and 1,000 mg O$_2$/L was a blend of solar and artificial radiation, considering the energetic needs across the year.

Finally, a variation of CPC called tubular reactor with an aperture and gross areas of 10 m^2 and 37.2 m^2 was respectively installed in a field test facility at Tyndall Air Force Base, Florida to tackle spiked water with BTEX in a recirculating batch mode (Vargas and Núñez, 2010). A total of 530 L of sieved groundwater was recycled with TiO$_2$ slurry and 100 mg/L of H$_2$O$_2$. The removal of 75% of BTEX was achieved after 3 h. Recently, Vargas et al. (2010), reported a tubular pilot plant (TPP) using slurry TiO$_2$ for the treatment of 15 L of contaminated water with industrial oil hydrocarbons (Vargas and Núñez, 2010). Dibenzothiophene (DBT) and naphthalene (NP) attained ~90% mineralization in 60 min when all pH values were tested; meanwhile, p-nitrophenol (PNP) reached ~40% in 180 min when pH = 6 and 10 were employed using slurry TiO$_2$.

Although CPC suffers from optical losses and tube aging (Malato et al., 2002; De Lasa et al., 2005), reactor clogging, catalyst fouling, the need for oxygen injection, and high pumping costs, it is still a fitting technology for pilot-scale and larger-scale operations. Extensive testing of photocatalysis and solar thermal engineering led to tremendous knowledge and understanding in the design and operation of photocatalytic systems incorporating CPC photoreactors, resulting in an attainable design and scaling-up of a plant based on such technology.

9.3 Inclined Plate Collectors

Inclined plate collectors (IPC) are flattened or curved panels that maintain a thin (about 1 mm) laminar flow of wastewater (normally 0.15–1.0 L/min). It offers the advantage of ensuring great mass transfer across various segments of the reactor throughout the large surface supporting the photocatalyst, in a structure known as a "thin-film fixed bed reactor" (TFFBR) (Ollis and Turchi, 1990; Fendrich et al., 2018). This configuration allows the non-concentrated photons to first travel throughout the reactant fluid before attaining the photocatalyst. Therefore, water overheating heating is not an issue (Tian et al., 2017). IPCs are perceived to be highly well suited to small-scale applications with limited amounts of fluid to be treated (Zhang et al., 2018). A schematic illustration of an IPC is shown in **Figure 9** (Fendrich et al., 2018).

Furthermore, the IPC may be closed or kept exposed to the atmosphere. When closed (flat plate reactor), they require purging with O$_2$ or supplying with oxidants, in addition to glazing. When exposed to the atmosphere (failing film reactor), purging reaction solution with air and oxygen becomes unnecessary, as further increased efficiency is realized by excluding reactor covering from absorbing light beams, and therefore eradicating the likely formation of a photocatalyst opaque film on the inner surface (Braham and Harris, 2009). However, during severe gusts, falling film reactors suffer from a loss of homogeneity and dryness of the catalysts (Bockelmann et al., 1995; Gernjak et al., 2004).

A TFFBR pilot plant was installed in a textile factory in Menzel Temime, Tunisia for the treatment of two commercial textile azo dyes using supported TiO$_2$ in a recirculating batch configuration. The pilot plant was composed of 2 reactors, each having a total illuminated area of 50 m^2 capable to treat a volume of 730 L. Seventy percent of degradation was attained in 8 h with an initial TOC in the water of 44.8 mg/L (Zayani et al., 2009).

9.4 Double-Skin Sheet Reactor

Originally reported by van Well et al. (1997), the engineering of a double-skin sheet reactor (DSSR) is straightforward (Van Well et al., 1997). DSSR is a non-concentrating reactor composed of commercial Plexiglas (transmission of light above 320 nm) double-skin sheet. It benefits from the employment of direct/diffuse radiation, as well as the maintenance of a turbulent flow regime that bypasses mass transfer boundaries between the photocatalyst and pollutants. However, it may be solely utilized in a low-throughput slurry mode, and it has low optical efficiency and bubble entrapment (De Lasa et al., 2005). Moreover, being a
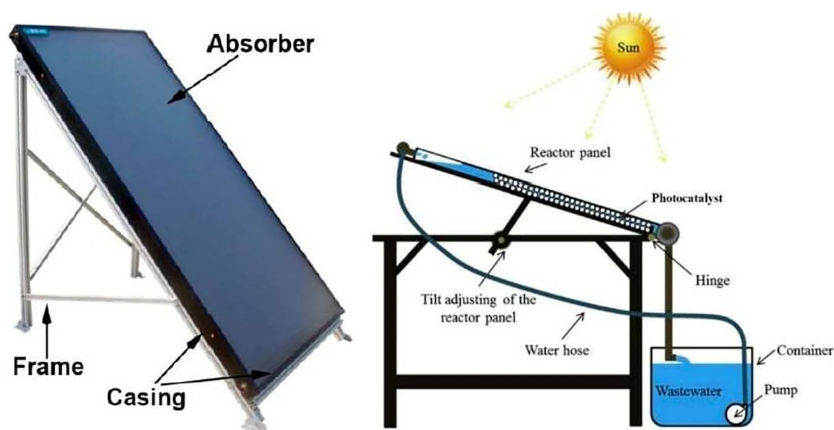
FIGURE 9 | Examples of inclined plate collectors prototype using TiO_2 nanoparticles coated on transparent beads for the remediation of methylene blue under solar illumination. Reproduced with permission (Fendrich et al., 2018).

closed reactor, it needs purging of reaction solution with O_2 or supplementing with additional oxidants (Bahnemann, 1999), which makes them unsuitable for commercialization. It was demonstrated that the present photocatalytic process using DSSR is inapt for tackling a large volume of effluent water. For instance, the projected areas necessary to decrease TOCs to 5% out of their initial concentration in 100 m^3/day of effluents were extremely large and unviable, spanning from 5,350 m^2 for lubricating oil effluent to a huge 106,100 m^2 for chlorinated organics effluent (Gulyas et al., 2005).

Nonetheless, a pilot plant composed of 12 DSSRs (2.45 m × 0.94 m) working in a recirculating batch mode with an overall surface area of 27.6 m^2 and loaded with 5 g/L of TiO2 was installed in 1998 at the Volkswagen plant in Wolfsburg to handle 500 L/day of treated wastewater *via* biological approaches. The

reduction of TOC reached 40% after 5.5 h beneath UV-solar irradiation (13.3 W/m^2) (Dillert et al., 1999).

9.5 Step Photoreactor

The cascade falling film principle is used in the step photoreactor to ensure adequate sunlight exposure and oxygenation of the effluent to be treated. The STEP solar reactor (**Figure 10**) is composed of a rectangular (2 m × 0.5 m = 1 m^2) 70-mm-high stainless-steel staircase vessel with 21 steps (Malato et al., 2007). To prevent water evaporation, it has a Pyrex glass (UV-transparent) lid. For the degradation of 4-chlorophenol, formetanate, and dyes, such reactors are set on a stationary rack inclined at 37°C, Almeria's latitude. The photocatalyst-support sheet was 1.36 m^2 in size. Twenty-five liters of DI water with the specified organic compounds was cycled in the
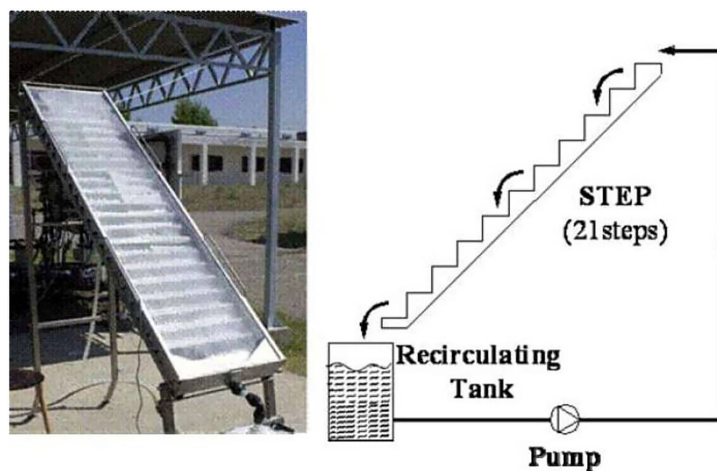

FIGURE 10 | Non-concentrating STEP solar collector tested at Platforma Solar de Almeria (SPAIN). Reproduced with permission (Malato et al., 2007).

dark at 7.5 L min^{-1} at the start of the experiment. For the entire degradation of 4-chlorophenol and formetanate, the STEP solar reactor was shown to be as competent as the CPC. In STEP reactor trials, however, both dyes took more time to be treated. The reactor was used to treat 25 L of water in a recirculating batch configuration. This setup was utilized to treat 25 L of an aqueous pesticide mixture with an initial TOC concentration of 8 mg/L in a recirculating batch mode. Exposed to a UV-A intensity of 30 W/m^2, 80% degradation was obtained in 4.5 h (Chan et al., 2001). However, owing to high capital costs caused primarily by the cover material, in addition to film problems, the need for reaction solution purging with O$_2$ or oxidant supplementation, and regular cleaning requirements, the STEP reactor became problematic for scale-up and commercialization. An example of a STEP reactor constructed at the PSA is shown in **Figure 10**. The major types of pilot-scale photoreactors are listed in **Table 5**.

To our knowledge, a pilot-scale photocatalytic reactor for the degradation of MPs does not exist yet. However, we took a big step in this framework during the CLAIM H2020 EU project where we successfully implemented a lab-scale photocatalytic reactor for the degradation of invisible MPs such as PP, PE, PVC, and nylon. For instance, 2 weeks of visible light irradiation of PP MPs resulted in a 65% decrease in average particle volume. The successful outcomes of the experimental work prove the efficiency of the designed reactors and suggest their prospects for employment in scaled-up water and wastewater treatment.

Finally, it should be noted that other reactor designs are proposed in the literature to treat wastewater but are not attractive for scale-up and commercialization due to the above-mentioned disadvantages: the use of the laminar flow regime, the need to purge with oxygen or to supply oxidants, the

requirement of additional support for glazing, high cost, low optical efficiency, the need for a tracking sunlight system, mechanical aspects, and climatic conditions. These reactors include the slurry bubble column reactor (used to treat nitrobenzene, chlorobenzene, and phenol) (Kamble et al., 2004), the flat plate column reactor (used for tackling aqueous solution of methylene blue) (Vaiano et al., 2015b), the pebble bed photoreactor (used for tackling water containing dye molecules) (Rao et al., 2012), the flat-packed bed reactor (used for the remediation of DI water inoculated with *Escherichia coli*) (Hanaor and Sorrell, 2014), the optical fiber photoreactors (used to treat 4-chlorophenol) (Peill and Hoffmann, 1997), and the fountain/water bell photocatalytic reactor and the rotating disk reactor (Braham and Harris, 2009).

10 CONCLUSIONS

This review examined the applications of AOPs, more specifically photocatalysis and Fenton processes, coupled with other techniques for the treatment of recalcitrant organic molecules and MPs. The efficiency of these technologies is mainly related to the generation of ROS such as OH$^•$, HO$_2$, and O$_2^-$, inducing the degradation of the polymeric chains in MPs. TiO$_2$ and ZnO in the form of nanoparticles, nanotubes, and nanorods are by far the most widely used photocatalysts for the degradation of the major types of MPs such as PE, PP, PVC, nylons, and others in the form of nanocomposites, films, or powders. The general mechanism of photocatalytic degradation of MPs involves the following steps: initiation, chain propagation, chain branching, chain scission, and termination.

TABLE 5 | Major types of pilot-scale photoreactors.

Reactor type	Total Aperture Area (m^2)	Pollutants	Type of Photocatalyst	Location	References
Parabolic Trough Reactors	29.2–465	Salicylic acid, trichloroethylene, tetrachloroethylene, chloroform, trichloroethane, carbon tetrachloride, methylene chloride, pentachlorophenol, oxalic acid, and 2,4-chlorophenol	TiO$_2$ slurry	New Mexico (SNL) Plataforma Solar de Almeria (PSA)	Malato et al. (2007) (Malato et al., 2007) Malato et al. (2002) (Malato et al., 2002)
Compound Parabolic Concentrator	8.9–150	Dichlorophenol, bacteria, dye effluents, pharmaceuticals, municipal wastewater, pesticides, chlorinated industrial water contaminants, paper mill effluents; surfactants, α-methylphenylglycine, commercial pesticides, BTEX, landfill leachates, Dibenzothiophene (DBT), naphthalene (NP), p-nitrophenol (PNP)	TiO$_2$ photo-Fenton reagents, photo-Fenton/aerobic biological system	Plataforma Solar de Almeria (PSA) HIDROCEN, Madrid Tyndall Air Force Base, Florida	Malato et al. (1997) (Malato et al., 1997) Blanco-Galvez et al. (2007) (Blanco-Galvez et al., 2007) Vargas et al. (2010) (Vargas and Núñez, 2010)
Inclined Plate Collectors	50	Commercial textile azo dyes	TiO$_2$	Menzel Temime, Tunisia	Zayani et al. (2009) (Zayani et al., 2009)
Double-Skin Sheet Reactor	27.6	Lubricating oil refinery effluent, chlorinated organics, biologically pretreated wastewater	TiO$_2$	Volkswagen plant in Wolfsburg	Dillert et al. (1999) (Dillert et al., 1999)

Characterization techniques like mass balance, turbidimetry, COD, and TOC are widely used to determine the rate of the photocatalytic reaction. The physicochemical, thermal, and mechanical properties of MPs are usually obtained through a large number of methods such as GPC, NMR, XPS (elemental composition), SEM, TEM (morphology), DSC, TGA (thermal), UTM, and DMA (mechanical). Regarding the characterization of by-products, classic techniques like GC-MS, LC-MS, and FTIR are extensively reported. Until now, there are no notable studies on the use of photocatalytic reactors at the scale of a pilot plant for the degradation of MPs, and it was very important to review the scaling-up methods applied to some commercial photocatalytic reactors employed for tackling various organic molecules. To control the parameters affecting the performances of photocatalytic reactors on the industrial scale, the use of complex mathematical and numerical methods is often necessary. Among the described designs, CPC techniques are now best fitted for a pilot-scale setup and beyond. The design and scale-up of a photocatalytic plant for MPs degradation based on CPC are reasonably feasible due to the extensive knowledge and expertise in the development and implementation of photocatalytic-based CPCs in both photocatalysis and solar thermal engineering.

Finally, it has to be noted that the decision of applying AOP technologies at an industrial scale for MPs degradation is intimately related to the degradation rate of pollutants. More specifically, the plant's capital cost is proportionally affected by the degradation kinetics of the process (i.e., photo-Fenton and photocatalysis) and by the consumption of chemicals and materials (hydrogen peroxide and photocatalysts), which, in turn, are strongly reliant on the concentration and type of pollutants (Comninellis et al., 2008).

AUTHOR CONTRIBUTIONS

FUNDING

SUPPLEMENTARY MATERIAL

The Supplementary Material for this article can be found online at: https://www.frontiersin.org/articles/10.3389/fmars.2022.885614/full#supplementary-material

REFERENCES

Abbasi, S., Sarafraz-Yazdi, A., Amiri, A., and Ghaemi, F. (2018). Development of Novel Magnetic Solid-Phase Extraction Sorbent Based on Fe3O4/Carbon Nanosphere/Polypyrrole Composite and Their Application to the Enrichment of Polycyclic Aromatic Hydrocarbons From Water Samples Prior to GC–FID Analysis. *J. Iran. Chem. Soc.* 15 (1), 153–161. doi: 10.1007/s13738-017-1218-6

Adekoya, D.O., Tahir, M., and Amin, N.A.S. (2017). G-C3N4/(Cu/TiO2) Nanocomposite for Enhanced Photoreduction of CO2 to CH3OH and HCOOH Under UV/visible Light. *J. CO2 Utiliz.* 18, 261–274. doi: 10.1016/j.jcou.2017.02.004

Adesina, A. A. (2004). Industrial Exploitation of Photocatalysis: Progress, Perspectives and Prospects. *Catalys. Survey. Asia.* 8 (4), 265–273. doi: 10.1007/s10563-004-9117-0

Aguilar-Vega, M. (2013). "Structure and Mechanical Properties of Polymers," in *Handbook of Polymer Synthesis, Characterization, and Processing.* Eds. E. Saldívar-Guerra and E. Vivaldo-Lima (Hoboken, NJ, USA: John Wiley & Sons, Inc), 425–434. doi: 10.1002/9781118480793.ch21

Ahmed, B., Limem, E., Abdel-Wahab, A., and Nasr, B. (2011). Photo-Fenton Treatment of Actual Agro-Industrial Wastewaters. *Ind. Eng. Chem. Res.* 50 (11), 6673–6680. doi: 10.1021/ie200266d

Alfaifi, B., Ullah, H., Alfaifi, S., Tahir, A., and Mallick, T. (2018). Photoelectrochemical Solar Water Splitting: From Basic Principles to Advanced Devices. *Veruscri. Funct. Nanomater.* 2 (12), BDJOC3. doi: 10.22261/FNAN.BDJOC3

Alfano, O. M., Bahnemann, D., Cassano, A. E., Dillert, R., and Goslich, R. (2000). Photocatalysis in Water Environments Using Artificial and Solar Light. *Catalys. Today* 58 (2-3), 199–230. doi: 10.1016/s0920-5861(00)00252-2

Ali, S. S., Qazi, I. A., Arshad, M., Khan, Z., Voice, T. C., and Mehmood, C. (2016). Photocatalytic Degradation of Low Density Polyethylene (LDPE) Films Using Titania Nanotubes. *Environ. Nanotechnol. Monit. Manage.* 5, 44–53. doi: 10.1016/j.enmm.2016.01.001

Ali, M.E., Rahman, M.M., Sarkar, S.M., and Hamid, S.B.A. (2014). Heterogeneous Metal Catalysts for Oxidation Reactions. *J. Nanomater.* 2014, ID 192038. doi: 10.1155/2014/192038

Allé, P. H., Garcia-Muñoz, P., Adouby, K., Keller, N., and Robert, D. (2021). Efficient Photocatalytic Mineralization of Polymethylmethacrylate and Polystyrene Nanoplastics by Tio2/β-SiC Alveolar Foams. *Environ. Chem. Lett.* 19 (2), 1803–1808. doi: 10.1007/s10311-020-01099-2

Almond, J., Sugumaar, P., Wenzel, M. N., Hill, G., and Wallis, C. (2020). Determination of the Carbonyl Index of Polyethylene and Polypropylene Using Specified Area Under Band Methodology With ATR-FTIR Spectroscopy. *e-Polymers.* 20 (1), 369–381. doi: 10.1515/epoly-2020-0041

Alvarado-Rolon, O., Natividad, R., Romero, R., Hurtado, L., and Ramírez-Serrano, A. (2018). Modelling and Simulation of the Radiant Field in an Annular Heterogeneous Photoreactor Using a Four-Flux Model. *Int. J. Photoener.* 1678385, 1–16. doi: 10.1155/2018/1678385

Amat, A. M., Arques, A., López, F., and Miranda, M. A. (2005). Solar Photo-Catalysis to Remove Paper Mill Wastewater Pollutants. *Solar. Energy* 79 (4), 393–401. doi: 10.1016/j.solener.2005.02.021

Amat, A. M., Arques, A., Miranda, M. A., and Seguí, S. (2004). Photo-Fenton Reaction for the Abatement of Commercial Surfactants in a Solar Pilot Plant. *Solar. Energy* 77 (5), 559–566. doi: 10.1016/j.solener.2004.03.028

Andrade, J. D. (1985). *Surface and Interfacial Aspects of Biomedical Polymers: Volume 1 Surface Chemistry and Physics* (Boston, MA: Springer US).

Antonopoulou, M., Kosma, C., Albanis, T., and Konstantinou, L. (2021). An Overview of Homogeneous and Heterogeneous Photocatalysis Applications for the Removal of Pharmaceutical Compounds From Real or Synthetic Hospital Wastewaters Under Lab or Pilot Scale. *Sci. Total. Environ.* 765, 144163. doi: 10.1016/j.scitotenv.2020.144163

Ariza-Tarazona, M. C., Villarreal-Chiu, J. F., Barbieri, V., Siligardi, C., and Cedillo-González, E. I. (2019). New Strategy for Microplastic Degradation: Green

Photocatalysis Using a Protein-Based Porous N-TiO2 Semiconductor. *Ceram. Int.* 45 (7), 9618–9624. doi: 10.1016/j.ceramint.2018.10.208

Arslan-Alaton, I., Kabdaşlı, I., and Teksoy, S. (2007). Effect of Fenton's Treatment on the Biodegradability of Chromium-Complex Azo Dyes. *Water Sci. Technol.* 55 (12), 107–112. doi: 10.2166/wst.2007.388

Augugliaro, V., García-López, E., Loddo, V., Malato-Rodríguez, S., Maldonado, I., Marcì, G., et al. (2005). Degradation of Lincomycin in Aqueous Medium: Coupling of Solar Photocatalysis and Membrane Separation. *Solar. Energy* 79 (4), 402–408. doi: 10.1016/j.solener.2005.02.020

Augugliaro, V., Litter, M., Palmisano, L., and Soria, J. (2006). The Combination of Heterogeneous Photocatalysis With Chemical and Physical Operations: A Tool for Improving the Photoprocess Performance. *J. Photochem. Photobiol. C.: Photochem. Rev.* 7 (4), 127–144. doi: 10.1016/j.jphotochemrev.2006.12.001

Babuponnusami, A., and Muthukumar, K. (2014). A Review on Fenton and Improvements to the Fenton Process for Wastewater Treatment. *J. Environ. Chem. Eng.* 2 (1), 557–572. doi: 10.1016/j.jece.2013.10.011

Bagheri, M., and Mohseni, M. (2015). A Study of Enhanced Performance of VUV/UV Process for the Degradation of Micropollutants From Contaminated Water. *J. Hazard. Mater.* 294, 1–8. doi: 10.1016/j.jhazmat.2015.03.036

Bahnemann, D. (1999). "Photocatalytic Detoxification of Polluted Waters," in *The Handbook of Environmental Chemistry (Reactions and Processes)*, vol. 2. Ed. P. Boule (Berlin, Heidelberg: Springer). doi: 10.1007/978-3-540-69044-3_11

Bandala, E. R., Arancibia-Bulnes, C. A., Orozco, S. L., and Estrada, C. A. (2004). Solar Photoreactors Comparison Based on Oxalic Acid Photocatalytic Degradation. *Solar. Energy* 77 (5), 503–512. doi: 10.1016/j.solener.2004.03.021

Bandala, E. R., and Estrada, C. (2007). Comparison of Solar Collection Geometries for Application to Photocatalytic Degradation of Organic Contaminants. *J. Solar. Energy Eng.* 129 (1), 22–26. doi: 10.1115/1.2390986

Barlow, A., Lehrle, R. S., and Robb, J. C. (1961). Direct Examination of Polymer Degradation by Gas Chromatography: I. *Appl. To. Polym. Anal. Char. Polym.* 2, 27–40. doi: 10.1016/0032-3861(61)90005-2

Bautista, P., Mohedano, A. F., Gilarranz, M. A., Casas, J. A., and Rodriguez, J. J. (2007). Application of Fenton Oxidation to Cosmetic Wastewaters Treatment. *J. Hazard. Mater.* 143 (1-2), 128–134. doi: 10.1016/j.jhazmat.2006.09.004

Beltrán, F. J., González, M., Ribas, F. J., and Alvarez, P. (1998). Fenton Reagent Advanced Oxidation of Polynuclear Aromatic Hydrocarbons in Water. *Water, Air, & Soil Pollution* 105, 3-4, 685–700. doi: 10.1023/a:1005048206991

Beltrán-Heredia, J., Torregrosa, J., García, J., Dominguez, J. R., and Tierno, J. C. (2001). Degradation of Olive Mill Wastewater by the Combination of Fenton's Reagent and Ozonation Processes With an Aerobic Biological Treatment. *Water Sci. Technol.* 44 (5), 103–108. doi: 10.2166/wst.2001.0262

Berkani, M., Bouchareb, M. K., Bouhelassa, M., and Kadmi, Y. (2020). Photocatalytic Degradation of Industrial Dye in Semi-Pilot Scale Prototype Solar Photoreactor: Optimization and Modeling Using ANN and RSM Based on Box-Wilson Approach. *Top. Catalys.* 63, 964–975. doi: 10.1007/s11244-020-01320-0

Blanco-Galvez, J., Fernaíndez-Ibaínãez, P., and Malato-Rodriíguez, S. (2007). Solar Photocatalytic Detoxification and Disinfection of Water: Recent Overview. *Solar. Energy Eng.* 129 (1), 4–15. doi: 10.1115/1.2390948

Blanco, J., Malato, S., Fernández, P., Vidal, A., Morales, A., Trincado, P., et al. (1999). Compound Parabolic Concentrator Technology Development to Commercial Solar Detoxification Applications. *Solar. Energy* 67 (4-6), 317–330. doi: 10.1016/s0038-092x(00)00078-5

Bockelmann, D., Weichgrebe, D., Goslich, R., and Bahnemann, D. (1995). Concentrating Versus non-Concentrating Reactors for Solar Water Detoxification. *Solar. Energy Mater. Solar. Cells* 38 (1-4), 441–451. doi: 10.1016/0927-0248(95)00005-4

Bolton, J. R., Bircher, K. G., Tumas, W., and Tolman, C. A. (2001). Figures-Of-Merit for the Technical Development and Application of Advanced Oxidation Technologies for Both Electric- and Solar-Driven Systems (IUPAC Technical Report). *Pure. Appl. Chem.* 73 (4), 627–637. doi: 10.1351/pac200173040627

Bonnet, N. (2004). Some Trends in Microscope Image Processing. *Micron* 35 (8), 635–653. doi: 10.1016/j.micron.2004.04.006

Braham, R. J., and Harris, A. T. (2009). Review of Major Design and Scale-Up Considerations for Solar Photocatalytic Reactors. *Ind. Eng. Chem. Res.* 48 (19), 8890–8905. doi: 10.1021/ie900859z

Browne, M.A., Galloway, T.S., and Thompson, R.C. (2010). Spatial Patterns of Plastic Debris Along Estuarine Shorelines. *Environ. Sci. Technol.* 44 (9), 3404–3409. doi: 10.1021/es903784e

Burge, R. E., Browne, M. T., Charalambous, P., Clark, A., and Wu, J. K. (1982). Multiple Signals in STEM. *J. Microscop.* 127 (1), 47–60. doi: 10.1111/j.1365-2818.1982.tb00396.x

Cai, Q. Q., Lee, B. C. Y., Ong, S. L., and Hu, J. Y. (2021). Fluidized-Bed Fenton Technologies for Recalcitrant Industrial Wastewater Treatment-Recent Advances, Challenges and Perspective. *Water Res.* 190, 116692. doi: 10.1016/j.watres.2020.116692

Cao, Y., Zhao, M., Ma, X., Song, Y., Zuo, S., Li, H., et al. (2021). Critical Review on the Interactions of Microplastics With Heavy Metals: Mechanism and Their Combined Effect on Organisms and Humans. *Sci. Total. Environ.* 788, 147620. doi: 10.1016/j.scitotenv.2021.147620

Carraher, C. E. (2018). *Carraher's Polymer Chemistry. Tenth edition* (Boca Raton: CRC Press, Taylor & Francis Group).

Carriazo, J., Guélou, E., Barrault, J., Tatibouët, J. M., Molina, R., and Moreno, S. (2005). Catalytic Wet Peroxide Oxidation of Phenol by Pillared Clays Containing Al–Ce–Fe. *Water Res.* 39 (16), 3891–3899. doi: 10.1016/j.watres.2005.06.034

Cassano, A. E., and Alfano, O. M. (2000). Reaction Engineering of Suspended Solid Heterogeneous Photocatalytic Reactors. *Catalys. Today* 58 (2-3), 167–197. doi: 10.1016/s0920-5861(00)00251-0

Cassano, A. E., Martin, C. A., Brandi, R. J., and Alfano, O. M. (1995). Photoreactor Analysis and Design: Fundamentals and Applications. *Ind. Eng. Chem. Res.* 34 (7), 2155–2201. doi: 10.1021/ie00046a001

Celasco, E., Valente, I., Marchisio, D. L., and Barresi, A. A. (2014). Dynamic Light Scattering and X-Ray Photoelectron Spectroscopy Characterization of PEGylated Polymer Nanocarriers: Internal Structure and Surface Properties. *Langmuir* 30 (28), 8326–8335. doi: 10.1021/la501198v

Chan, A. H., Porter, J. F., Barford, J. P., and Chan, C. K. (2001). Photocatalytic Thin Film Cascade Reactor for Treatment of Organic Compounds in Wastewater. *Water Sci. Technol.* 44 (5), 187–195. doi: 10.2166/wst.2001.0283

Chen, G., Feng, Q., and Wang, J. (2020). Mini-Review of Microplastics in the Atmosphere and Their Risks to Humans. *Sci. Total. Environ.* 703, 135504. doi: 10.1016/j.scitotenv.2019.135504

Cho, S., and Choi, W. (2001). Solid-Phase Photocatalytic Degradation of PVC–TiO2 Polymer Composites. *J. Photochem. Photobiol. A.: Chem.* 143 (2–3), 221–228. doi: 10.1016/S1010-6030(01)00499-3

Chong, M. N., Jin, B., Chow, C. W. K., and Saint, C. (2010). Recent Developments in Photocatalytic Water Treatment Technology: A Review. *Water Res.* 44 (10), 0–3027. doi: 10.1016/j.watres.2010.02.039

Chung, Y.-H., Han, K., Lin, C.-Y., O'Neill, D., Mul, G., Mei, B., et al. (2019). Photocatalytic Hydrogen Production by Photo-Reforming of Methanol With One-Pot Synthesized Pt-Containing TiO2 Photocatalysts. *Catal. Today* 356, 95–100. doi: 10.1016/j.cattod.2019.07.042

Colburn, T. W., Toops, T. J., and Wereszczak, A. A. (2020). Industrial Scalable Additives for Enhanced Decomposition of Plastic Waste Through Photocatalysis. *Acad. J. Polymer Sci.*, 4(2) 555633. doi: 10.19080/AJOP.2020.04.555633. United States.

Comninellis, C., Kapalka, A., Malato, S., Parsons, S. A., Poulios, I., and Mantzavinos, D. (2008). Advanced Oxidation Processes for Water Treatment: Advances and Trends for R&D. *J. Chem. Technol. Biotechnol.* 83 (6), 769–776. doi: 10.1002/jctb.1873

Coronado, J. (2013). "Chapter 2 Photons, Electrons and Holes: Fundamentals of Photocatalysis With Semiconductor," in *Design of Advanced Photocatalytic Materials for Energy and Environmental Applications* London. Eds. J. Coronado, F. Fresno, M. D. Hernández-Alonso and R. Portela (London: Springer-Verlag), 5–34. ISBN 978-1-4471-5061-9. doi: 10.1007/978-1-4471-5061-9

Cox, K.D., Covernton, G.A., Davies, H.L., Dower, J.F., Juanes, F., and Dudas, S.E. (2019). Human Consumption of Microplastics. *Environ. Sci. Technol.* 53 (12), 7068–7074. doi: 10.1021/acs.est.9b01517

Cui, X., Li, W., Ryabchuk, P., Junge, K., and Beller, M. (2018). Bridging Homogeneous and Heterogeneous Catalysis by Heterogeneous Single-Metal-Site Catalysts. *Nat. Catalys.* 1 (6), 385–397. doi: 10.1038/s41929-018-0090-9

Danish, M. S. S., Estrella, L. L., Alemaida, I. M. A., Lisin, A., Moiseev, N., Ahmadi, M., et al. (2021). Photocatalytic Applications of Metal Oxides for Sustainable Environmental Remediation. *Metals* 11 (1), 80. doi: 10.3390/met11010080

De Andrade, P. M., Dufrayer, C. R., Ionashiro, E. Y., and De Brito, N. N. (2020). The Use of Metallurgical Waste for Heterogeneous Photo Fenton-Like Treatment of Cosmetic Effluent. *J. Environ. Chem. Eng.* 8 (5), 104148. doi: 10.1016/j.jece.2020.104148

De Lasa, H., Serrano, B., and Salaices, M. (2005). "Chapter 2: Novel Photocatalytic Reactors for Water and Air Treatment," in *Photocatalytic Reaction Engineering* (Boston, MA: Springer), 17–47. doi: 10.1007/0-387-27591-6_2

De los Santos-Villarreal, G., and Elizalde, L. E. (2013). "Polymer Spectroscopy and Compositional Analysis," in *In Handbook of Polymer Synthesis, Characterization, and Processing*. Eds. E. Saldívar-Guerra and E. Vivaldo-Lima (Hoboken, NJ, USA: John Wiley & Sons, Inc), 335–354. doi: 10.1002/9781118480793.ch16

Denny, F., Scott, J., Pareek, V., Ding Peng, G., and Amal, R. (2009). CFD Modelling for a TiO2-Coated Glass-Bead Photoreactor Irradiated by Optical Fibers: Photocatalytic Degradation of Oxalic Acid. *Chem. Eng. Sci.* 64 (8), 1695–1706. doi: 10.1016/j.ces.2008.12.021

Dey, T.K., Uddin, M.E., and Jamal, M. (2021). Detection and Removal of Microplastics in Wastewater: Evolution and Impact. *Environ. Sci. pollut. Res.* 28 (14), 16925–16947. doi: 10.1007/s11356-021-12943-5

Dillert, R., Cassano, A. E., Goslich, R., and Bahnemann, D. (1999). Large Scale Studies in Solar Catalytic Wastewater Treatment. *Catalys. Today* 54, 267–282. doi: 10.1016/S0920-5861(99)00188-1

Domínguez-Jaimes, L. P., Cedillo-González, E. I., Luévano-Hipólito, E., Acuña-Bedoya, J. D., and Hernández-López, J. M. (2021). Degradation of Primary Nanoplastics by Photocatalysis Using Different Anodized TiO2 Structures. *J. Hazard. Mater.* 413, 125452. doi: 10.1016/j.jhazmat.2021.125452

Eduardo da Hora Machado, A., Padovani Xavier, T., Rodrigues de Souza, D., Antonio de Miranda, J., Thomas Fleury Mendonça Duarte, E., Ruggiero, R., et al. (2004). Solar Photo-Fenton Treatment of Chip Board Production Waste Water. *Solar. Energy* 77 (5), 583–589. doi: 10.1016/j.solener.2004.03.024

Eriksen, M., Lebreton, L.C.M., Carson, H.S., Thiel, M., Moore, C.J., Borerro, J.C., et al. (2014). Plastic Pollution in the World's Oceans: More Than 5 Trillion Plastic Pieces Weighing Over 250,000 Tons Afloat at Sea. *PLoS One* 9 (12), e111913. doi: 10.1371/journal.pone.0111913

Evode, N., Qamar, S.A., Bilal, M., Barceló, D., and Iqbal, H.M.N. (2021). Plastic Waste and Its Management Strategies for Environmental Sustainability. *Case Stud. Chem. Environ. Eng.* 4, 100142. doi: 10.1016/j.cscee.2021.100142

Fagan, R., McCormack, D. E., Dionysiou, D. D., and Pillai, S. C. A. (2016). Review of Solar and Visible Light Active TiO2 Photocatalysis for Treating Bacteria, Cyanotoxins and Contaminants of Emerging Concern. *Mater. Sci. Semiconduct. Process.* 42 (1), 2–14. doi: 10.1016/j.mssp.2015.07.052

Falconer, J. L., and Magrini-Bair, K. A. (1998). Photocatalytic and Thermal Catalytic Oxidation of Acetaldehyde on Pt/Tio2. *J. Catalys.* 179 (1), 171–178. doi: 10.1006/jcat.1998.2215

Fallmann, H., Krutzler, T., Bauer, R., Malato, S., and Blanco, J. (1999). Applicability of the Photo-Fenton Method for Treating Water Containing Pesticides. *Catalys. Today* 54 (2-3), 309–319. doi: 10.1016/s0920-5861(99)00192-3

Fendrich, M., Quaranta, A., Orlandi, M., Bettonte, M., and Miotello, A. (2018). Solar Concentration for Wastewaters Remediation: A Review of Materials and Technologies. *Appl. Sci.* 9 (1), 118. doi: 10.3390/app9010118

Fenton, H.J.H. (1894). LXXIII.—Oxidation of Tartaric Acid in Presence of Iron. *J. Chem. Soc.* 65, 899–910. doi: 10.1039/ct8946500899

Fernández, P., Blanco, J., Sichel, C., and Malato, S. (2005). Water Disinfection by Solar Photocatalysis Using Compound Parabolic Collectors. *Catalys. Today* 101 (3-4), 345–352. doi: 10.1016/j.cattod.2005.03.062

Filho, H. J. I., Siqueira, A. F., Alcântara, M. A. K., Aguiar, L. G., Da Rós, P. C. M., Napoleão, D.A.d. S., et al. (2021). Solar Photo-Fenton Oxidation of Mature Landfill Leachate: Empirical Model and Chemical Inferences. *Environ. Technol.* 7 (1), 015519. doi: 10.1080/09593330.2021.1909656

Frias, J.P.G.L., and Nash, R. (2019). Microplastics: Finding a Consensus on the Definition. *Mar. pollut. Bull.* 138, 145–147. doi: 10.1016/j.marpolbul.2018.11.022

Galloway, J. A., Montminy, M. D., and Macosko, C. W. (2002). Image Analysis for Interfacial Area and Cocontinuity Detection in Polymer Blends. *Polymer* 43 (17), 4715–4722. doi: 10.1016/S0032-3861(02)00282-3

Gamaralalage, D., Sawai, O., and Nunoura, T. (2019). Degradation Behavior of Palm Oil Mill Effluent in Fenton Oxidation. *J. Hazard. Mater.* 364, 791–799. doi: 10.1016/j.jhazmat.2018.07.023

Ganguly, P., Panneri, S., Hareesh, U. S., Breen, A., and Pillai, S.C. (2019). "Chapter 23 - Recent Advances in Photocatalytic Detoxification of Water. In Micro and Nano Technologies," in *Nanoscale Materials in Water Purification* Elsevier. Eds. S. Thomas, D. Pasquini, S.-Y. Leu and D. A. Gopakumar (Elsevier), 653–688. doi: 10.1016/B978-0-12-813926-4.00029-X

Gaya, U. I., and Abdullah, A. H. (2008). Heterogeneous Photocatalytic Degradation of Organic Contaminants Over Titanium Dioxide: A Review of Fundamentals, Progress and Problems. *J. Photochem. Photobiol. C.: Photochem. Rev.* 9 (1), 1–12. doi: 10.1016/j.jphotochemrev.2007.12.003

Gernjak, W., Maldonado, M. I., Malato, S., Cáceres, J., Krutzler, T., Glaser, A., et al. (2004). Pilot-Plant Treatment of Olive Mill Wastewater (OMW) by Solar TiO2 Photocatalysis and Solar Photo-Fenton. *Solar. Energy* 77 (5), 567–572. doi: 10.1016/j.solener.2004.03.030

Geyer, R., Jambeck, J.R., and Law, K.L. (2017). Production, Use, and Fate of All Plastics Ever Made. *Sci. Adv.* 3 (7), e1700782. doi: 10.1126/sciadv.1700782

Ghafoori, S., Mehrvar, M., and Chan, P. K. (2014). Photoreactor Scale-Up for Degradation of Aqueous Poly(Vinyl Alcohol) Using UV/H2O2 Process. *Chem. Eng. J.* 245, 133–142. doi: 10.1016/j.cej.2014.01.055

Gill, P., Moghadam, T. T., and Ranjbar, B. (2010). Differential Scanning Calorimetry Techniques: Applications in Biology and Nanoscience. *J. Biomolecul. Technique.* 21 (4), 167–193.

Giroto, J. A., Teixeira, A. C. S. C., Nascimento, C. A. O., and Guardani, R. (2010). Degradation of Poly(Ethylene Glycol) in Aqueous Solution by Photo-Fenton and H2O2/UV Processes. *Ind. Eng. Chem. Res.* 49 (7), 3200–3206. doi: 10.1021/ie9015792

Goswami, D. Y. (1997). A Review of Engineering Developments of Aqueous Phase Solar Photocatalytic Detoxification and Disinfection Processes. *J. Solar. Energy Eng.* 119 (2), 101–107. doi: 10.1115/1.2887886

Goswami, D. Y., Vijayaraghavan, S., Lu, S., and Tamm, G. (2004). New and Emerging Developments in Solar Energy. *Solar. Energy* 76 (1-3), 33–43. doi: 10.1016/s0038-092x(03)00103-8

Gregory, J. (1998). Turbidity and Beyond. *Filtrat. Separat.* 35 (1), 63–67. doi: 10.1016/S0015-1882(97)83117-5

Guillard, C., Lachheb, H., Houas, A., Ksibi, M., Elaloui, E., and Herrmann, J.-M. (2003). Influence of Chemical Structure of Dyes, of pH and of Inorganic Salts on Their Photocatalytic Degradation by TiO2 Comparison of the Efficiency of Powder and Supported Tio2. *J. Photochem. Photobiol. A.: Chem.* 158 (1), 27–36. doi: 10.1016/s1010-6030(03)00016-9

Gulkaya, İ, Surucu, G. A., and Dilek, F. B. (2006). Importance of H2O2/Fe2+ Ratio in Fenton's Treatment of a Carpet Dyeing Wastewater. *J. Hazard. Mater.* 136 (3), 763–769. doi: 10.1016/j.jhazmat.2006.01.006

Gulshan, F., Yanagida, S., Kameshima, Y., Isobe, T., Nakajima, A., and Okada, K. (2010). Various Factors Affecting Photodecomposition of Methylene Blue by Iron-Oxides in an Oxalate Solution. *Water Res.* 44 (9), 2876–22884. doi: 10.1016/j.watres.2010.01.040

Gulyas, H., Jain, H. B., Susanto, A. L., Malekpur, M., Harasiuk, K., Krawczyk, I., et al. (2005). Solar Photocatalytic Oxidation of Pretreated Wastewaters: Laboratory Scale Generation Of Design Data for Technical-Scale Double-Skin Sheet Reactors. *Envi. Technol.* 26 (5), 501–514. doi: 10.1080/09593332608618540

Gutierrez-Mata, A. G., Velazquez-Martínez, S., Álvarez-Gallegos, A., Ahmadi, M., Hernández-Pérez, JoséA., Ghanbari, F., et al. (2017). Recent Overview of Solar Photocatalysis and Solar Photo-Fenton Processes for Wastewater Treatment. *Int. J. Photoener.* 8528063, 1–27. doi: 10.1155/2017/8528063

Habib, I.Y., Burhan, J., Jaladi, F., Lim, C.M., Usman, A., Kumara, N. T. R. N., et al. (2020). Effect of Cr Doping in CeO2 Nanostructures on Photocatalysis and H2O2 Assisted Methylene Blue Dye Degradation. *Catalys. Today* 375, 506-513. doi: 10.1016/j.cattod.2020.04.008. ISSN 0920-5861.

Hakkarainen, M., and Karlsson, S. (2006). "Gas Chromatography in Analysis of Polymers and Rubbers," in *Encyclopedia of Analytical Chemistry*. Ed. R. A. Meyers (Chichester, UK: John Wiley & Sons, Ltd), a2010. doi: 10.1002/9780470027318.a2010

Hale, R.C., Seeley, M.E., La Guardia, M.J., Mai, L., and Zeng, E.Y.A. (2020). Global Perspective on Microplastics. *J. Geophys. Res.: Ocean.* 125 (1), e2018JC014719. doi: 10.1029/2018JC014719

Hamd, W.S., and Dutta, J. (2020). "Chapter 11 - Heterogeneous Photo-Fenton Reaction and its Enhancement Upon Addition of Chelating Agents," in *Nanomaterials for the Detection and Removal of Wastewater Pollutants, A Volume in Micro and Nano Technologies*. Eds. B. Bonelli, F. S. Freyria, I. Rossetti and R. Sethi (Amsterdam Oxford Cambridge, MA: Elsevier), 303–330. ISBN 9780128184899. doi: 10.1016/B978-0-12-818489-9.00011-6

Hanaor, D. A. H., and Sorrell, C. C. (2014). Sand Supported Mixed-Phase TiO2 Photocatalysts for Water Decontamination Applications: Sand Supported Mixed-Phase TiO2 Photocatalysts. *Adv. Eng. Mater.* 16 (2), 248–254. doi: 10.1002/adem.201300259

Hartmann, N.B., Hüffer, T., Thompson, R.C., Hassellöv, M., Verschoor, A., Daugaard, A.E., et al. (2019). Are We Speaking the Same Language? Recommendations for a Definition and Categorization Framework for Plastic Debris. *Environ. Sci. Technol.* 53 (3), 1039–1047. doi: 10.1021/acs.est.8b05297

He, D., Luo, Y., Lu, S., Liu, M., Song, Y., and Lei, L. (2018). Microplastics in Soils: Analytical Methods, Pollution Characteristics and Ecological Risks. *TrAC. Trends Anal. Chem.* 109, 163–172. doi: 10.1016/j.trac.2018.10.006

Herrmann, J.-M. (1999). Heterogeneous Photocatalysis: Fundamentals and Applications to the Removal of Various Types of Aqueous Pollutants. *Catalys. Today* 53 (1), 115–129. doi: 10.1016/s0920-5861(99)00107-8

Herrmann, J.-M., and Guillard, C. (2000). Photocatalytic Degradation of Pesticides in Agricultural Used Waters. *Compt. Rendus. l'Académie. Des. Sci. - Ser. IIC. – Chem.* 3 (6), 417–422. doi: 10.1016/S1387-1609(00)01137-3

He, J., Yang, X., Men, B., and Wang, D. (2015). Interfacial Mechanisms of Heterogeneous Fenton Reactions Catalyzed by Iron-Based Materials: A Review. *J. Environ. Sci.* 39, 97–109. doi: 10.1016/j.jes.2015.12.003

He, J., Yang, X., Men, B., Yu, L., and Wang, D. (2015). EDTA Enhanced Heterogeneous Fenton Oxidation of Dimethyl Phthalate Catalyzed by Fe3O4: Kinetics and Interface Mechanism. *J. Mol. Catalys. A.: Chem.* 408, 179–188. doi: 10.1016/j.molcata.2015.07.030

Hodson, M.E., Duffus-Hodson, C.A., Clark, A., Prendergast-Miller, M.T., and Thorpe, K.L. (2017). Plastic Bag Derived-Microplastics as a Vector for Metal Exposure in Terrestrial Invertebrates. *Environ. Sci. Technol.* 51 (8), 4714–4721. doi: 10.1021/acs.est.7b00635

Hoffmann, M.R., Martin, S.T., and Choi, W. (1995). Environmental Applications of Semiconductor Photocatalysis. *Chem. Rev.* 95 (1), 69–96. doi: 10.1021/cr00033a004

Huang, W., Brigante, M., Wu, F., Hanna, K., and Mailhot, G. (2013). Effect of Ethylenediamine-N,N′-Disuccinic Acid on Fenton and Photo-Fenton Processes Using Goethite as an Iron Source: Optimization of Parameters for Bisphenol A Degradation. *Environ. Sci. pollut. Res.* 20 (1), 39–50. doi: 10.1007/s11356-012-1042-6

Huang, H.-H., Lu, M.-C., and Chen, J.-N. (2001). Catalytic Decomposition of Hydrogen Peroxide and 2-Chlorophenol With Iron Oxides. *Water Res.* 35 (9), 2291–2299. doi: 10.1016/s0043-1354(00)00496-6

Izunobi, J. U., and Higginbotham, C. L. (2011). Polymer Molecular Weight Analysis by 1H NMR Spectroscopy. *J. Chem. Educ.* 88 (8), 1098–1104. doi: 10.1021/ed100461v

Jamali, A., Vanraes, R., Hanselaer, P., and Van Gerven, T. (2013). A Batch LED Reactor for the Photocatalytic Degradation of Phenol. *Chem. Eng. Process.: Process.* 71, 43–50. doi: 10.1016/j.cep.2013.03.010

Jiang, R., Lu, G., Yan, Z., Liu, J., Wu, D., and Wang, Y. (2021). Microplastic Degradation by Hydroxy-Rich Bismuth Oxychloride. *J. Hazard. Mater.* 405, 124247. doi: 10.1016/j.jhazmat.2020.124247

Kamble, S. P., Sawant, S. B., and Pangarkar, V. G. (2004). Novel Solar-Based Photocatalytic Reactor for Degradation of Refractory Pollutants. *AIChE. J.* 50 (7), 1647–1650. doi: 10.1002/aic.10125

Kaur, R., and Kaur, H. (2021). Solar Driven Photocatalysis - an Efficient Method for Removal of Pesticides From Water and Wastewater. *Biointerfac. Res. Appl. Chem.* 11 (12), 9071–9084. doi: 10.33263/BRIAC112.90719084

Kim, J. R., and Kan, E. (2015). Heterogeneous Photo-Fenton Oxidation of Methylene Blue Using CdS-Carbon Nanotube/TiO2 Under Visible Light. *J. Ind. Eng. Chem.* 21, 644–652. doi: 10.1016/j.jiec.2014.03.032

Kim, S., Sin, A., Nam, H., Park, Y., Lee, H., and Han, C. (2022). Advanced Oxidation Processes for Microplastics Degradation: A Recent Trend. *Chem. Eng. J. Adv.* 9, 100213. doi: 10.1016/j.ceja.2021.100213

Knoblauch, D., Mederake, L., and Stein, U. (2018). Developing Countries in the Lead—What Drives the Diffusion of Plastic Bag Policies? *Sustainability* 10 (6), 1994. doi: 10.3390/su10061994

Konstas, K., and Konstantinou, A. (2019). Photocatalytic Treatment of Pharmaceuticals in Real Hospital Wastewaters for Effluent Quality Amelioration. *Water* 11 (10), 2165. doi: 10.3390/w11102165

Kositzi, M., Poulios, I., Malato, S., Caceres, J., and Campos, A. (2004). Solar Photocatalytic Treatment of Synthetic Municipal Wastewater. *Water Res.* 38 (5), 1147–1154. doi: 10.1016/j.watres.2003.11.024

Kumar, J., and Bansal, A. (2013). Photocatalytic Degradation in Annular Reactor: Modelization and Optimization Using Computational Fluid Dynamics (CFD) and Response Surface Methodology (RSM). *J. Environ. Chem. Eng.* 1 (3), 398–405. doi: 10.1016/j.jece.2013.06.002

Kumar, A. P., Depan, D., Singh Tomer, N., and Singh, R. P. (2009). Nanoscale Particles for Polymer Degradation and Stabilization—Trends and Future Perspectives. *Prog. Polym. Sci.* 34 (6), 479–515. doi: 10.1016/j.progpolymsci.2009.01.002

Kwan, W. P., and Voelker, B. M. (2003). Rates of Hydroxyl Radical Generation and Organic Compound Oxidation in Mineral-Catalyzed Fenton-Like Systems. *Environ. Sci. Technol.* 37 (6), 1150–1158. doi: 10.1021/es020874g

Lasee, S., Mauricio, J., Thompson, W.A., Karnjanapiboonwong, A., Kasumba, J., Subbiah, S., et al. (2017). Microplastics in a Freshwater Environment Receiving Treated Wastewater Effluent: Microplastics in Urban Surface Water. *Integrat. Environ. Assess. Manage.* 13 (3), 528–532. doi: 10.1002/ieam.1915

Law, K.L., and Thompson, R.C. (2014). Microplastics in the Seas. *Science* 345 (6193), 144–145. doi: 10.1126/science.1254065

Lebreton, L., and Andrady, A. (2019). Future Scenarios of Global Plastic Waste Generation and Disposal. *Palgrave. Commun.* 5 (1), 6. doi: 10.1057/s41599-018-0212-7

Lee, J.-M., Busquets, R., Choi, I.-C., Lee, S.-H., Kim, J.-K., and Campos, L. C. (2020). Photocatalytic Degradation of Polyamide 66; Evaluating the Feasibility of Photocatalysis as a Microfibre-Targeting Technology. *Water* 12, 3551. doi: 10.3390/w12123551

Lee, H.-J., Lee, H., and Lee, C. (2014). Degradation of Diclofenac and Carbamazepine by the Copper(II)-Catalyzed Dark and Photo-Assisted Fenton-Like Systems. *Chem. Eng. J.* 245, 258–264. doi: 10.1016/j.cej.2014.02.037

Liang, W., Luo, Y., Song, S., Dong, X., and Yu, X. (2013). High Photocatalytic Degradation Activity of Polyethylene Containing Polyacrylamide Grafted Tio2. *Polym. Degrad. Stab.* 98 (9), 1754–1761. doi: 10.1016/j.polymdegradstab.2013.05.027

Liao, Q., Sun, J., and Gao, L. (2009). Degradation of Phenol by Heterogeneous Fenton Reaction Using Multi-Walled Carbon Nanotube Supported Fe2O3 Catalysts. *Colloid. Surf. A.: Physicochem. Eng. Aspect.* 345 (1-3), 95–100. doi: 10.1016/j.colsurfa.2009.04.037

Lin, S.-S., and Gurol, M. D. (1998). Catalytic Decomposition of Hydrogen Peroxide on Iron Oxide: Kinetics, Mechanism, and Implications. *Environ. Sci. Technol.* 32 (10), 1417–1423. doi: 10.1021/es970648k

Li Puma, G. (2005). Dimensionless Analysis of Photocatalytic Reactors Using Suspended Solid Photocatalysts. *Inst. Chem. Engi.* 83 (7), 820–826. doi: 10.1205/cherd.04336

Liu, R., Chiu, H. M., Shiau, C.-S., Yeh, R. Y.-L., and Hung, Y.-T. (2007). Degradation and Sludge Production of Textile Dyes by Fenton and Photo-Fenton Processes. *Dyes. Pigment.* 73 (1), 1–6. doi: 10.1016/j.dyepig.2005.10.002

Liu, Y., Jin, W., Zhao, Y., Zhang, G., and Zhang, W. (2017). Enhanced Catalytic Degradation of Methylene Blue by α-Fe2O3/graphene Oxide *via* Heterogeneous Photo-Fenton Reactions. *Appl. Catalys. B.: Environ.* 206, 642–652. doi: 10.1016/j.apcatb.2017.01.075

Liu, P., Qian, L., Wang, H., Zhan, X., Lu, K., Gu, C., et al. (2019). New Insights Into Aging Behavior of Microplastics Accelerated by Advanced Oxidation Processes. *Environ. Sci. Technol.* 53 (7), 3579–3588. doi: 10.1021/acs.est.9b00493

Liu, W., Zhang, J., Liu, H., Guo, X., Zhang, X., Yao, X., et al. (2021). Review of the Removal of Microplastics in Global Wastewater Treatment Plants: Characteristics and Mechanisms. *Environ. Int.* 146, 106277. doi: 10.1016/j.envint.2020.106277

Li, S., Xu, S., He, L., Xu, F., Wang, Y., and Zhang, L. (2020). Photocatalytic Degradation of Polyethylene Plastic With Polypyrrole/TiO2 Nanocomposite as

Photocatalyst. *Polymer-Plast. Technol. Eng.* 49 (4), 400–406. doi: 10.1080/03602550903532166

Llorente-García, B. E., Hernández-López, J. M., Zaldívar-Cadena, A. A., Siligardi, C., and Cedillo-González, E. I. (2020). First Insights Into Photocatalytic Degradation of HDPE and LDPE Microplastics by a Mesoporous N–TiO2 Coating: Effect of Size and Shape of Microplastics. *Coatings.* 10 (7), 658. doi: 10.3390/coatings10070658

Lum, P.T., Foo, K.Y., Zakaria, N.A., and Palaniandy, P. (2019). Ash Based Nanocomposites for Photocatalytic Degradation of Textile Dye Pollutants: A Review. *Mater. Chem. Phys.* 241, 122405. doi: 10.1016/j.matchemphys.2019.122405

Luna, A. J., Chiavone-Filho, O., Machulek, A., de Moraes, J. E. F., and Nascimento, C. A. O. (2012). Photo-Fenton Oxidation of Phenol and Organochlorides (2,4-DCP and 2,4-D) in Aqueous Alkaline Medium With High Chloride Concentration. *J. Environ. Manage.* 111, 10–17. doi: 10.1016/j.jenvman.2012.06.014

Luo, H., Xiang, Y., Li, Y., Zhao, Y., and Pan, X. (2021). Photocatalytic Aging Process of Nano-TiO2 Coated Polypropylene Microplastics: Combining Atomic Force Microscopy and Infrared Spectroscopy (AFM-IR) for Nanoscale Chemical Characterization. *J. Hazard. Mater.* 404, 124159. doi: 10.1016/j.jhazmat.2020.124159

Machado, A. E. H., De Miranda, J. A., De Freitas, R. F., Duarte, E. T. F. M., Ferreira, L. F., Albuquerque, Y. D. T., et al. (2003). Destruction of the Organic Matter Present in Effluent From a Cellulose and Paper Industry Using Photocatalysis. *J. Photochem. Photobiol. A.: Chem.* 155 (1-3), 231–241. doi: 10.1016/s1010-6030(02)00393-3

Malato, S., Blanco, J., Alarcón, D. C., Maldonado, M. I., Fernández-Ibáñez, P., and Gernjak, W. (2007). Photocatalytic Decontamination and Disinfection of Water With Solar Collectors. *Catalys. Today* 122 (1-2), 137–149. doi: 10.1016/j.cattod.2007.01.034

Malato, S., Blanco, J., Richter, C., Curcó, D., and Gimenez, J. (1997). Low-Concentrating CPC Collectors for Photocatalytic Water Detoxification: Comparison With a Medium Concentrating Solar Collector. *Water Sci. Technol.* 35 (4), 157–164. doi: 10.1016/s0273-1223(97)00021-8

Malato, S., Blanco, J., Vidal, A., Fernández, P., Cáceres, J., Trincado, P., et al. (2002). New Large Solar Photocatalytic Plant: Set-Up and Preliminary Results. *Chemosphere* 47 (3), 235–240. doi: 10.1016/s0045-6535(01)00220-x

Martínez, N. S. S., Fernández, J. F., Segura, X. F., and Ferrer, A. S. (2003). Pre-Oxidation of an Extremely Polluted Industrial Wastewater by the Fenton's Reagent. *J. Hazard. Mater.* 101 (3), 315–322. doi: 10.1016/s0304-3894(03)00207-3

Martínez-Huitle, C. A., Rodrigo, M. A., Sirés, I., and Scialdone, O. (2015). Single and Coupled Electrochemical Processes and Reactors for the Abatement of Organic Water Pollutants: A Critical Review. *Chem. Rev.* 115 (24), 13362–13407. doi: 10.1021/acs.chemrev.5b00361

Martínez, S., Morales-Mejía, J. C., Hernández, P. P., Santiago, L., and Almanza, R. (2014). Solar Photocatalytic Oxidation of Triclosan With TiO2 Immobilized on Volcanic Porous Stones on a CPC Pilot Scale Reactor. *Energy Proc.* 57, 3014–3020. doi: 10.1016/j.egypro.2014.10.337

Ma, B., Xue, W., Hu, C., Liu, H., Qu, J., and Li, L. (2019). Characteristics of Microplastic Removal *via* Coagulation and Ultrafiltration During Drinking Water Treatment. *Chem. Eng. J.* 359, 159–167. doi: 10.1016/j.cej.2018.11.155

McLoughlin, O. A., Kehoe, S. C., McGuigan, K. G., Duffy, E. F., Al Touati, F., Gernjak, W., et al. (2004a). Solar Disinfection of Contaminated Water: A Comparison of Three Small-Scale Reactors. *Solar. Energy* 77 (5), 657–664. doi: 10.1016/j.solener.2004.07.004

McLoughlin, O. A., Kehoe, S. C., McGuigan, K. G., Duffy, E. F., Al Touati, F., Gernjak, W., et al. (2004b). Solar Disinfection of Contaminated Water: A Comparison of Three Small-Scale Reactors. *Solar. Energy* 77 (5), 657–664. doi: 10.1016/j.solener.2004.07.004

Medeiros, P. M. (2018). "Gas Chromatography–Mass Spectrometry (GC–MS)," in *Encyclopedia of Geochemistry*. Ed. W. M. White (Cham: Springer International Publishing), 530–535. Encyclopedia of Earth Sciences Series. doi: 10.1007/978-3-319-39312-4_159

Meeker, R. E.United States Patent Office (1963). *Stabilization of Hydrogen Peroxide* (US). (Patent number: US3208825A).

Mehos, M., Turchi, C., Pacheco, J., Boegel, A. J., Merrill, T., and Stanley, R. (1992). *Pilot-Scale Study of the Solar Detoxification of VOC-Contaminated*

Groundwater* (United States: U.S. Department of Energy Office of Scientific and Technical Information). Available at: https://www.osti.gov/biblio/7102976-pilot-scale-study-solar-detoxification-voc-contaminated-groundwater.

Menard, K. P., and Menard, N. R. (2020). *Dynamic Mechanical Analysis. 3rd ed* (Boca Raton: CRC Press). doi: 10.1201/9780429190308

Miao, F., Liu, Y., Gao, M., Yu, X., Xiao, P., Wang, M., et al. (2020). Degradation of Polyvinyl Chloride Microplastics *via* an Electro-Fenton-Like System With a TiO2/graphite Cathode. *J. Hazard. Mater.* 399, 123023. doi: 10.1016/j.jhazmat.2020.123023

Minero, C., Pelizzetti, E., Malato, S., and Blanco, J. (1993). Large Solar Plant Photocatalytic Water Decontamination: Degradation of Pentachlorophenol. *Chemosphere* 26 (12), 0–2119. doi: 10.1016/0045-6535(93)90337-5

Miranda-García, N., Suárez, S., Sánchez, B., Coronado, J. M., Malato, S., and Maldonado, M. I. (2001). Photocatalytic Degradation of Emerging Contaminants in Municipal Wastewater Treatment Plant Effluents Using Immobilized TiO2 in a Solar Pilot Plant. *Appl. Catalys. B.: Environ.* 103 (3-4), 294–301. doi: 10.1016/j.apcatb.2011.01.030

Mishra, M., and Chun, D.-M. (2015). α-Fe2O3 as a Photocatalytic Material: A Review. *Appl. Catalys. A.* 498, 126–141. doi: 10.1016/j.apcata.2015.03.023

Moghaddami, M., and Raisee, M. (2012). Performance and Energy Consumption Analysis of UV-H2O2 Photoreactors Using Computational Fluid Dynamics. *Int. J. Environ. Sci. Dev.* 3 (4), 387–392. doi: 10.7763/IJESD.2012.V3.253

Mohamed, A.S., AbuKhadra, M.R., Abdallah, E.A., El-Sherbeeny, A.M., and Mahmoud, R.K. (2020). The Photocatalytic Performance of Silica Fume Based Co3O4/MCM-41 Green Nanocomposite for Instantaneous Degradation of Omethoate Pesticide Under Visible Light. *J. Photochem. Photobiol. A.* 392, 112434. doi: 10.1016/j.jphotochem.2020.112434

Mohamed, A., Yousef, S., Nasser, W. S., Osman, T. A., Knebel, A., Valadez Sánchez, E. P., et al. (2020). Rapid Photocatalytic Degradation of Phenol From Water Using Composite Nanofibers Under UV. *Environ. Sci. Eur.* 32, 160. doi: 10.1186/s12302-020-00436-0

Mokhbi, Y., Korichi, M., and Akchiche, Z. (2019). Combined Photocatalytic and Fenton Oxidation for Oily Wastewater Treatment. *Appl. Water Sci.* 9 (2), 35–44. doi: 10.1007/s13201-019-0916-x

Molina, C. B., Sanz-Santos, E., Boukhemkhem, A., Bedia, J., Belver, C., and Rodriguez, J. (2020). Removal of Emerging Pollutants in Aqueous Phase by Heterogeneous Fenton and Photo-Fenton With Fe2O3- TiO2-Clay Heterostructures. *Environ. Sci. pollut. Res.* 27, 38434–38445. doi: 10.1007/s11356-020-09236-8

Moreira, J., Serrano, B., Ortiz, A., and De Lasa, H. (2010). Evaluation of Photon Absorption in an Aqueous TiO2 Slurry Reactor Using Monte Carlo Simulations and Macroscopic Balance. *Ind. Eng. Chem. Res.* 49 (21), 10524–10534. doi: 10.1021/ie100374f

Motaung, T. E., Luyt, A. S., Bondioli, F., Messori, M., Saladino, M. L., Spinella, A., et al. (2012). PMMA–Titania Nanocomposites: Properties and Thermal Degradation Behaviour. *Polym. Degrad. Stab.* 97 (8), 1325–1333. doi: 10.1016/j.polymdegradstab.2012.05.022

Mozia, S., Brożek, P., Przepiórski, J., Tryba, B., and Morawski, A. W. (2012). Immobilized TiO2 for Phenol Degradation in a Pilot-Scale Photocatalytic Reactor. *J. Nanomater.* 2012, 1–10. doi: 10.1155/2012/949764

Mumford, A.C., Barringer, J.L., Benzel, W.M., Reilly, P.A., and Young, L.Y. (2012). Microbial Transformations of Arsenic: Mobilization From Glauconitic Sediments to Water. *Water Res.* 46 (9), 2859–2868. doi: 10.1016/j.watres.2012.02.044

Murphy, F., Ewins, C., Carbonnier, F., and Quinn, B. (2016). Wastewater Treatment Works (WwTW) as a Source of Microplastics in the Aquatic Environment. *Environ. Sci. Technol.* 50 (11), 5800–5808. doi: 10.1021/acs.est.5b05416

Nabi, I., Bacha, A.-U.-R, Ahmad, F., and Zhang, L. (2021). Application of Titanium Dioxide for the Photocatalytic Degradation of Macro- and Micro-Plastics: A Review. *J. Environ. Chem. Eng.* 9 (5), 105964. doi: 10.1016/j.jece.2021.105964

Nabi, I., Bacha, A.-U.-R, Li, K., Cheng, H., Wang, T., Liu, Y., et al. (2020). Complete Photocatalytic Mineralization of Microplastic on TiO2 Nanoparticle Film. *iScience.* 23 (7), 101326. doi: 10.1016/j.isci.2020.101326

Nadeem, N., Zahid, M., Tabasum, A., Mansha, A., Jilani, A., Bhatti, I. A., et al. (2020). Degradation of Reactive Dye Using Heterogeneous Photo-Fenton

Catalysts: ZnFe2O4 and GO-ZnFe2O4 Composite. *Mater. Res. Exp.* 7 (1), 015519. doi: 10.1088/2053-1591/ab66ee

Nakano, K., Obuchi, E., Takagi, S., Yamamoto, R., Tanizaki, T., Taketomi, M., et al. (2004). Photocatalytic Treatment of Water Containing Dinitrophenol and City Water Over Tio2/Sio2. *Separat. Purifi. Technol.* 34 (1-3), 67–72. doi: 10.1016/s1383-5866(03)00176-x

Navntoft, C., Araujo, P., Litter, M. I., Apella, M. C., Fernández, D., Puchulu, M. E., et al. (2007). Field Tests of the Solar Water Detoxification SOLWATER Reactor in Los Pereyra, Tucumán, Argentina. *J. Solar. Energy Eng.* 129 (1), 127–134. doi: 10.1115/1.2391318

Oller, I., Gernjak, W., Maldonado, M. I., Pérez-Estrada, L. A., Sánchez-Pérez, J. A., and Malato, S. (2006). Solar Photocatalytic Degradation of Some Hazardous Water-Soluble Pesticides at Pilot-Plant Scale. *J. Hazard. Mater.* 138 (3), 507–517. doi: 10.1016/j.jhazmat.2006.05.075

Ollis, D. F., and Turchi, C. (1990). Heterogeneous Photocatalysis for Water Purification: Contaminant Mineralization Kinetics and Elementary Reactor Analysis. *Envi. Prog.* 9 (4), 229–234. doi: 10.1002/ep.670090417

Oyama, T., Aoshima, A., Horikoshi, S., Hidaka, S., Zhao, J., and Serpone, N. (2004). Solar Photocatalysis, Photodegradation of a Commercial Detergent in Aqueous TiO2 Dispersions Under Sunlight Irradiation. *Solar. Energy* 77 (5), 525–532. doi: 10.1016/j.solener.2004.04.020

Padervand, M., Lichtfouse, E., Robert, D., and Wang, C. (2020). Removal of Microplastics From the Environment. A Review. *Environ. Chem. Lett.* 18 (3), 807–828. doi: 10.1007/s10311-020-00983-1

Parra, S., Malato, S., Blanco, J., Péringer, P., and Pulgari, C. (2001). Concentrating Versus Non-Concentrating Reactors for Solar Photocatalytic Degradation of P-Nitrotoluene-O-Sulfonic Acid. *Water Sci. Technol.* 44 (5), 219–227. doi: 10.2166/wst.2001.0290

Pawar, R. C., and Lee, C. S. (2015). "Heterogeneous Photocatalysts Based on Organic/Inorganic Semiconductor," in *Heterogeneous Nanocomposite-Photocatalysis for Water Purification* (Elsevier: Elsevier), 43–96. doi: 10.1016/B978-0-323-39310-2.00003-5

Peill, N. J., and Hoffmann, M. R. (1997). Solar-Powered Photocatalytic Fiber-Optic Cable Reactor for Waste Stream Remediation. *J. Solar. Energy Eng.* 119 (3), 229–236. doi: 10.1115/1.2888024

Perez, E. R., Knapp, J. A., Horn, C. K., Stillman, S. L., Evans, J. E., and Arfsten, D. P. (2016). Comparison of LC–MS-MS and GC–MS Analysis of Benzodiazepine Compounds Included in the Drug Demand Reduction Urinalysis Program. *J. Anal. Toxicol.* 40 (3), 201–207. doi: 10.1093/jat/bkv140

Porta, R. (2021). Anthropocene, the Plastic Age and Future Perspectives. *FEBS Open Bio* 11 (4), 948–953. doi: 10.1002/2211-5463.13122

Potakis, N., Frontistis, Z., Antonopoulou, M., Konstantinou, I., and Mantzavinos, D. (2017). Oxidation of Bisphenol A in Water by Heat-Activated Persulfate. *J. Environ. Manage.* 195 (2), 125–132. doi: 10.1016/j.jenvman.2016.05.045

Pozzo, R. L., Giombi, J. L., Baltanás, M. A., and Cassano, A. E. (2000). The Performance in a Fluidized Bed Reactor of Photocatalysts Immobilized Onto Inert Supports. *Catalys. Today* 62 (2-3), 175–187. doi: 10.1016/s0920-5861(00)00419-3

Prairie, M. R., Pacheco, J., and Evans, L. R. (1991). *Solar Detoxification of Water Containing Chlorinated Solvents and Heavy Metals via TiO2 Photocatalysis* (United States). Available at: https://www.osti.gov/biblio/5858147-solar-detoxification-water-containing-chlorinated-solvents-heavy-metals-via-tio-sub-photocatalysis.

Prieto, O., Fermoso, J., Nuñez, Y., Del Valle, J. L., and Irusta, R. (2005). Decolouration of Textile Dyes in Wastewaters by Photocatalysis With Tio2. *Solar. Energy* 79 (4), 376–383. doi: 10.1016/j.solener.2005.02.023

Qiu, Q., Peng, J., Yu, X., Chen, F., Wang, J., and Dong, F. (2015). Occurrence of Microplastics in the Coastal Marine Environment: First Observation on Sediment of China. *Mar. pollut. Bull.* 98 (1–2), 274–280. doi: 10.1016/j.marpolbul.2015.07.028

Rabek Jan, F. (2012). *Polymer Photodegradation: Mechanisms and Experimental Methods* (Dordrecht: Springer Netherlands).

Rajamanickam, D., and Shanthi, M. (2016). Photocatalytic Degradation of an Organic Pollutant by Zinc Oxide – Solar Process. *Arab. J. Chem.* 9, S1858–S1868. doi: 10.1016/j.arabjc.2012.05.006

Raji, M., Mirbagheri, S. A., Ye, F., and Dutta, J. (2021). Nano Zero-Valent Iron on Activated Carbon Cloth Support as Fenton-Like Catalyst for Efficient Color

and COD Removal From Melanoidin Wastewater. *Chemosphere* 263, 127945. doi: 10.1016/j.chemosphere.2020.127945

Rao, N. N., Chaturvedi, V., and Li Puma, G. (2012). Novel Pebble Bed Photocatalytic Reactor for Solar Treatment of Textile Wastewater. *Chem. Eng. J.* 184, 90–97. doi: 10.1016/j.cej.2012.01.004

Remucal, C. K., and Sedlak, D. L. (2011). "The Role of Iron Coordination in the Production of Reactive Oxidants From Ferrous Iron Oxidation by Oxygen and Hydrogen Peroxide," in *In ACS Symposium Series*, vol. 1071 . Eds. P. G. Tratnyek, T. J. Grundl and S. B. Haderlein (Washington, DC: American Chemical Society), 177–197. doi: 10.1021/bk-2011-1071.ch009

Revel, M., Châtel, A., and Mouneyrac, C. (2018). Micro(Nano)Plastics: A Threat to Human Health? *Curr. Opin. Environ. Sci. Health* 1, 17–23. doi: 10.1016/j.coesh.2017.10.003

Rist, S., Carney Almroth, B., Hartmann, N.B., and Karlsson, T.M.A. (2018). Critical Perspective on Early Communications Concerning Human Health Aspects of Microplastics. *Sci. Total. Environ.* 626, 720–726. doi: 10.1016/j.scitotenv.2018.01.092

Rivas, F. J., Beltrán, F. J., Gimeno, O., and Alvarez, P. (2003). Treatment of Brines by Combined Fenton's Reagent–Aerobic Biodegradation: II. Process Modelling. *J. Hazardous Mat.* 96, 2-3, 259–276. doi: 10.1016/s0304-3894(02)00216-9

Rivas, F. J., Beltrán, F. J., Gimeno, O., and Frades, J. (2001). Treatment of Olive Oil Mill Wastewater by Fenton's Reagent. *J. Agric. Food Chem.* 49 (4), 1873–1880. doi: 10.1021/jf001223b

Rossetti, G. H., Albizzati, E. D., and Alfano, O. M. (2004). Modeling of a Flat-Plate Solar Reactor. Degradation of Formic Acid by the Photo-Fenton Reaction. *Solar. Energy* 77 (5), 461–470. doi: 10.1016/j.solener.2004.04.019

RuÃz-Delgado, A., Roccamante, M. A., Malato, S., Agüera, A., and Oller, I. (2020). Olive Mill Wastewater Reuse to Enable Solar Photo-Fenton-Like Processes for the Elimination of Priority Substances in Municipal Wastewater Treatment Plant Effluents. *Environ. Sci. pollut. Res.* 27, 38148–38154. doi: 10.1007/s11356-020-09721-0

Sacco, O., Vaiano, V., and Sannino, D. (2020). Main Parameters Influencing the Design of Photocatalytic Reactors for Wastewater Treatment: A Mini Review. *J. Chem. Technol. Biotechnol.* 95 (10), 2608–2618. doi: 10.1002/jctb.6488

Sagawe, G., Lehnard, A., Lübber, M., and Bahnemann, D. (2001). The Insulated Solar Fenton Hybrid Process: Fundamental Investigations. *HCA.* 84 (12), 3742–3759. doi: 10.1002/1522-2675(20011219)84:12<3742::aid-hlca3742>3.0.co;2-q

Saggioro, E. M., Oliveira, A. S., Buss, D. F., Magalhães D. de, P., Pavesi, T., Jimenéz, M., et al. (2015). Photo-Decolorization and Ecotoxicological Effects of Solar Compound Parabolic Collector Pilot Plant and Artificial Light Photocatalysis of Indigo Carmine Dye. *Dyes. Pigment.* 113, 571–580. doi: 10.1016/j.dyepig.2014.09.029

Salgado, P., Frontela, J. L., and Vidal, G. (2020). Optimization of Fenton Technology for Recalcitrant Compounds and Bacteria Inactivation. *Catalysts* 10 (12), 1483. doi: 10.3390/catal10121483

Samet, Y., Ayadi, M., and Abdelhedi, R. (2009). Degradation of 4-Chloroguaiacol by Dark Fenton and Solar Photo-Fenton Advanced Oxidation Processes. *Water Environ. Res.* 81 (12), 2389–2397. doi: 10.2175/106143009x425997

Sanchez, W., Bender, C., and Porcher, J.-M. (2014). Wild Gudgeons (Gobio Gobio) From French Rivers Are Contaminated by Microplastics: Preliminary Study and First Evidence. *Environ. Res.* 128, 98–100. doi: 10.1016/j.envres.2013.11.004

Sangami, S., and Manu, B. (2017). Optimization of Fenton's Oxidation of Herbicide Dicamba in Water Using Response Surface Methodology. *Appl. Water Sci.* 7, 4269–4280. doi: 10.1007/s13201-017-0559-8

Santos-Juanes, L., Sánchez, J. L. G., López, J. L. C., Oller, I., Malato, S., and Sánchez Pérez, J. A. (2011). Dissolved Oxygen Concentration: A Key Parameter in Monitoring the Photo-Fenton Process. *Appl. Catalys. B.: Environ.* 104 (3–4), 316–323. doi: 10.1016/j.apcatb.2011.03.013

Saravanan, A., Kumar, P.S., Vo, D.-V. N., Yaashikaa, P.R., Karishma, S., Jeevanantham, S., et al. (2020). Photocatalysis for Removal of Environmental Pollutants and Fuel Production: A Review. *Environ. Chem. Lett* 19(1), 441-463. doi: 10.1007/s10311-020-01077-8. IF 5.922.

Sarria, V., Péringer, P., Cáceres, J., Blanco, J., Malato, S., and Pulgarin, C. (2004). Solar Degradation of 5-Amino-6-Methyl-2-Benzimidazolone by TiO2 and

Iron(III) Catalyst With H2O2 and O2 as Electron Acceptors. *Energy* 29 (5-6), 853–860. doi: 10.1016/s0360-5442(03)00190-7

Sarwan, B., Acharya, A. D., Kaur, S., and Pare, B. (2020). Visible Light Photocatalytic Deterioration of Polystyrene Plastic Using Supported BiOCl Nanoflower and Nanodisk. *Eur. Polym. J.* 134, 109793. doi: 10.1016/j.eurpolymj.2020.109793

Sattler, C., De Oliveira, L., Tzschirner, M., and Machado, A. E. H. (2004). Solar Photocatalytic Water Detoxification of Paper Mill Effluents. *Energy* 29 (5-6), 835–843. doi: 10.1016/s0360-5442(03)00189-0

Satuf, M. L., Brandi, R. J., Cassano, A. E., and Alfano, O. M. (2007). Scaling-Up of Slurry Reactors for the Photocatalytic Degradation of 4-Chlorophenol. *Catalys. Today* 129 (1–2), 110–117. doi: 10.1016/j.cattod.2007.06.056

Sekar, R., and DiChristina, T. J. (2017). Degradation of the Recalcitrant Oil Spill Components Anthracene and Pyrene by a Microbially Driven Fenton Reaction. *FEMS Microbiol. Lett.* 364 (21), fnx203 . doi: 10.1093/femsle/fnx203

Serrano, B., and De Lasa, H. (1997). Photocatalytic Degradation of Water Organic Pollutants. Kinetic Modeling and Energy Efficiency. *Ind. Eng. Chem. Res.* 36 (11), 4705–4711. doi: 10.1021/ie970104r

Shang, J., Chai, M., and Zhu, Y. (2003). Photocatalytic Degradation of Polystyrene Plastic Under Fluorescent Light. *Environ. Sci. Technol.* 37 (19), 4494–4499. doi: 10.1021/es0209464

Silva, T. F. C. V., Soares, P. A., Manenti, D. R., Fonseca, A., Saraiva, I., Boaventura, R. A. R., et al. (2017). An Innovative Multistage Treatment System for Sanitary Landfill Leachate Depuration: Studies at Pilot-Scale. *Sci. Total. Environ.* 576, 99–117. doi: 10.1016/j.scitotenv.2016.10.058

Singa, P. K., Isa, M. H., Lim, J.-W., Ho, Y.-C., and Krishnan, S. (2021). Photo-Fenton Process for Removal of Polycyclic Aromatic Hydrocarbons From Hazardous Waste Landfill Leachate. *Int. J. Environ. Sci. Technol.* 18 (11), 3515–3526. doi: 10.1007/s13762-020-03010-6

Singh, B., and Sharma, N. (2008). Mechanistic Implications of Plastic Degradation. *Polym. Degrad. Stab.* 93 (3), 561–584. doi: 10.1016/j.polymdegradstab.2007.11.008

Sivagami, K., Anand, D., Divyapriya, G., and Nambi, I. (2019). Treatment of Petroleum Oil Spill Sludge Using the Combined Ultrasound and Fenton Oxidation Process. *Ultrasonic. Sonochem.* 51, 340–349. doi: 10.1016/j.ultsonch.2018.09.007

Sol, D., Laca, A., Laca, A., and Díaz, M. (2021). Microplastics in Wastewater and Drinking Water Treatment Plants: Occurrence and Removal of Microfibres. *Appl. Sci.* 11 (21), 10109. doi: 10.3390/app112110109

Song, W., Cheng, M., Ma, J., Ma, W., Chen, C., and Zhao, J. (2006). Decomposition of Hydrogen Peroxide Driven by Photochemical Cycling of Iron Species in Clay. *Environ. Sci. Technol.* 40 (15), 4782–4787. doi: 10.1021/es060624q

Sun, J., Dai, X., Wang, Q., van Loosdrecht, M.C.M., and Ni, B.-J. (2019). Microplastics in Wastewater Treatment Plants: Detection, Occurrence and Removal. *Water Res.* 152, 21–37. doi: 10.1016/j.watres.2018.12.050

Talvitie, J., Mikola, A., Koistinen, A., and Setälä, O. (2017). Solutions to Microplastic Pollution – Removal of Microplastics From Wastewater Effluent With Advanced Wastewater Treatment Technologies. *Water Res.* 123, 401–407. doi: 10.1016/j.watres.2017.07.005

Tang, W. Z., and Huang, C. P. (1996). 2,4-Dichlorophenol Oxidation Kinetics by Fenton's Reagent. *Environ. Technol.* 17 (12), 1371–1378. doi: 10.1080/09593330.1996.9618465

Tanveer, M., and Tezcanli Guyer, G. (2013). Solar Assisted Photo Degradation of Wastewater by Compound Parabolic Collectors: Review of Design and Operational Parameters. *Renewable Sustain. Energy Rev.* 24, 534–543. doi: 10.1016/j.rser.2013.03.053

Tapia, J. B., Haines, J., Yapor, J. P., and Reynolds, M. M. (2019). Identification of the Degradation Products of a Crosslinked Polyester Using LC-Ms. *Polym. Degrad. Stab.* 168, 108948. doi: 10.1016/j.polymdegradstab.2019.108948

Tejera, J., Hermosilla, D., Gascó, A., Miranda, R., Alonso, V., Negro, C., et al. (2021). Treatment of Mature Landfill Leachate by Electrocoagulation Followed by Fenton or UVA-LED Photo-Fenton Processes. *J. Tai. Insti. Chem. Engi.* 119, 33–44. doi: 10.1016/j.jtice.2021.02.018

Thompson, R.C., Olsen, Y., Mitchell, R.P., Davis, A., Rowland, S.J., John, A.W.G., et al. (2004). Lost at Sea: Where Is All the Plastic? *Science* 304 (5672), 838–838. doi: 10.1126/science.1094559

Tian, L., Chen, Q., Jiang, W., Wang, L., Xie, H., Kalogerakis, N., et al. (2019). A Carbon-14 Radiotracer-Based Study on the Phototransformation of Polystyrene Nanoplastics in Water Versus in Air. *Environ. Sci.: Nano.* 6 (9), 2907–2917. doi: 10.1039/C9EN00662A

Tian, Z., Perers, B., Furbo, S., and Fan, J. (2017). Annual Measured and Simulated Thermal Performance Analysis of a Hybrid Solar District Heating Plant With Flat Plate Collectors and Parabolic Trough Collectors in Series. *Appl. Energy* 205, 417–427. doi: 10.1016/j.apenergy.2017.07.139

Tofa, T. S. (2018). Degradation of Microplastic Residuals in Water by Visible Light Photocatalysis. Thesis, Number: 18493, Series: TRITA-ABE-MBT (Sweden: KTH, Sustainable development, Environmental science and Engineering). Available at: http://www.diva-portal.org/smash/get/diva2:1266570/FULLTEXT01.pdf.

Tofa, T. S., Kunjali, K. L., Paul, S., Kunjali, K. L., and Dutta, J. (2019). Visible Light Photocatalytic Degradation of Microplastic Residues With Zinc Oxide Nanorods. *Environ. Chem. Lett.* 17, 1341–1346. doi: 10.1007/s10311-019-00859-z

Tofa, T. S., Ye, F., Kunjali, K. L., and Dutta, J. (2019). Enhanced Visible Light Photodegradation of Microplastic Fragments With Plasmonic Platinum/Zinc Oxide Nanorod Photocatalysts. *Catalysts.* 9 (10), 819. doi: 10.3390/catal9100819

Tong, H., Ouyang, S., Bi, Y., Umezawa, N., Oshikiri, M., and Ye, J. (2012). Nano-Photocatalytic Materials: Possibilities and Challenges. *Adv. Mater.* 24 (2), 229–251. doi: 10.1002/adma.201102752

Uheida, A., Mejía, H. G., Abdel-Rehim, M., Hamd, W., and Dutta, J. (2020). Visible Light Photocatalytic Degradation of Polypropylene Microplastics in a Continuous Water Flow System. *J. Hazard. Mater.* 406, 124299. doi: 10.1016/j.jhazmat.2020.124299

Ul haq, I., Ahmad, W., Ahmad, I., and Yaseen, M. (2020). Photocatalytic Oxidative Degradation of Hydrocarbon Pollutants in Refinery Wastewater Using TiO2 as Catalyst. *Water Environ. Res.* 92 (12), 2086–2094. doi: 10.1002/wer.1370

Vaiano, V., Sacco, O., Pisano, D., Sannino, D., and Ciambelli, P. (2015a). From the Design to the Development of a Continuous Fixed Bed Photoreactor for Photocatalytic Degradation of Organic Pollutants in Wastewater. *Chem. Eng. Sci.* 137, 152–160. doi: 10.1016/j.ces.2015.06.023

Vaiano, V., Sacco, O., Pisano, D., Sannino, D., and Ciambelli, P. (2015b). From the Design to the Development of a Continuous Fixed Bed Photoreactor for Photocatalytic Degradation of Organic Pollutants in Wastewater. *Chem. Eng. Sci.* 137, 152–160. doi: 10.1016/j.ces.2015.06.023

Vaiano, V., Sacco, O., and Sannino, D. (2019). Electric Energy Saving in Photocatalytic Removal of Crystal Violet Dye Through the Simultaneous Use of Long-Persistent Blue Phosphors, Nitrogen-Doped TiO2 and UV-Light Emitting Diodes. *J. Clean. Product.* 210, 1015–1021. doi: 10.1016/j.jclepro.2018.11.017

Van Well, M., Dillert, R. H. G., Bahnemann, D. W., Benz, V. W., and Mueller, M. A. A. (1997). Novel Nonconcentrating Reactor for Solar Water Detoxification. *J. Solar. Energy Eng.* 119, 114–119. doi: 10.1115/1.2887888

Vargas, V., and Núñez, O. (2010). Photocatalytic Degradation of Oil Industry Hydrocarbons Models at Laboratory and at Pilot-Plant Scale. *Solar. Energy* 84 (2), 345–351. doi: 10.1016/j.solener.2009.12.005

Venkataramana, C., Botsa, S. M., Shyamala, P., and Muralikrishna, R. (2021). Photocatalytic Degradation of Polyethylene Plastics by NiAl2O4 Spinels-Synthesis and Characterization. *Chemosphere* 265, 129021. doi: 10.1016/j.chemosphere.2020.129021

Vione, D., Minella, M., Maurino, V., and Minero, C. (2014). Indirect Photochemistry in Sunlit Surface Waters: Photoinduced Production of Reactive Transient Species. *Chem. - A. Eur. J.* 20 (34), 10590–10606. doi: 10.1002/chem.2014004

Vital-Grappin, A. D., Ariza-Tarazona, M. C., Luna-Hernández, V. M., Villarreal-Chiu, J. F., Hernández-López, J. M., Siligardi, C., et al. (2021). The Role of the Reactive Species Involved in the Photocatalytic Degradation of HDPE Microplastics Using C,N- TiO2 Powders. *Polymers* 13 (7), 999. doi: 10.3390/polym13070999

Walling, C. (1975). Fenton's Reagent Revisited. *Acc. Chem. Res.* 84, 125–131. doi: 10.1021/ar50088a003

Wang, S. (2008). A Comparative Study of Fenton and Fenton-Like Reaction Kinetics in Decolourisation of Wastewater. *Dyes. Pigment.* 76 (3), 714–720. doi: 10.1016/j.dyepig.2007.01.012

Wang, W., Ndungu, A.W., Li, Z., and Wang, J. (2017). Microplastics Pollution in Inland Freshwaters of China: A Case Study in Urban Surface Waters of Wuhan, China. *Sci. Total. Environ.* 575, 1369–1374. doi: 10.1016/j.scitotenv.2016.09.213

Wang, H., Wang, H.-L., Jiang, W.-F., and Li, Z.-Q. (2009). Photocatalytic Degradation of 2,4-Dinitrophenol (DNP) by Multi-Walled Carbon Nanotubes (MWCNTs)/ TiO2 Composite in Aqueous Solution Under Solar Irradiation. *Water Res.* 43 (1), 204–210. doi: 10.1016/j.watres.2008.10.003

Wright, S.L., Thompson, R.C., and Galloway, T.S. (2013). The Physical Impacts of Microplastics on Marine Organisms: A Review. *Environ. pollut.* 178, 483–492. doi: 10.1016/j.envpol.2013.02.031

Xu, C., Anusuyadevi, P. R., Aymonier, C., Luque, R., and Marre, S. (2019). Nanostructured Materials for Photocatalysis. *Chem. Soc. Rev.* 48 (14), 3868–3902. doi: 10.1039/C9CS00102F

Xue, W., Peng, Z., Huang, D., Zeng, G., Wan, J., Xu, R., et al. (2018). Nanoremediation of Cadmium Contaminated River Sediments: Microbial Response and Organic Carbon Changes. *J. Hazard. Mater.* 359, 290–299. doi: 10.1016/j.jhazmat.2018.07.062

Xu, Q., Huang, Q.-S., Luo, T.-Y., Wu, R.-L., Wei, W., and Ni, B.-J. (2021). Coagulation Removal and Photocatalytic Degradation of Microplastics in Urban Waters. *Chem. Eng. J.* 416, 129123. doi: 10.1016/j.cej.2021.129123

Yadav, R., Amoli, V., Singh, J., Tripathi, M.K., Bhanja, P., Bhaumik, A., et al. (2018). Plasmonic Gold Deposited on Mesoporous TixSi1–xO2 With Isolated Silica in Lattice: An Excellent Photocatalyst for Photocatalytic Conversion of CO2 Into Methanol Under Visible Light Irradiation. *J. CO2 Utiliz.* 27, 11–21. doi: 10.1016/j.jcou.2018.06.016

Yousif, E., and Haddad, R. (2013). Photodegradation and Photostabilization of Polymers, Especially Polystyrene: Review. *SpringerPlus* 2 (1), 398. doi: 10.1186/2193-1801-2-398

Zapata, A., Malato, S., Sánchez-Pérez, J. A., Oller, I., and Maldonado, M. I. (2010). Scale-Up Strategy for a Combined Solar Photo-Fenton/biological System for Remediation of Pesticide-Contaminated Water. *Catalys. Today* 151 (1-2), 100–106. doi: 10.1016/j.cattod.2010.01.034

Zayani, G., Bousselmi, L., Mhenni, F., and Ghrabi, A. (2009). Solar Photocatalytic Degradation of Commercial Textile Azo Dyes: Performance of Pilot Plant Scale Thin Film Fixed-Bed Reactor. *Desalination* 246 (1-3), 344–352. doi: 10.1016/j.desal.2008.03.059

Zhang, M.-h., Dong, H., Zhao, L., Wang, D.-X., and Meng, D. (2019). A Review on Fenton Process for Organic Wastewater Treatment Based on Optimization Perspective. *Sci. Total. Environ.* 670, 110–121. doi: 10.1016/j.scitotenv.2019.03.180

Zhang, Y., Sivakumar, M., Yang, S., Enever, K., and Ramezanianpour, M. (2018). Application of Solar Energy in Water Treatment Processes: A Review. *Desalination* 428, 116–145. doi: 10.1016/j.desal.2017.11.020

Zhang, J., Tian, B., Wang, L., Xing, M., and Lei, J. (2018). *Photocatalysis: Fundamentals, Materials and Applications* (Singapor: Springer Verlag). ISBN: 9789811321122,9811321124.

Zhao, X. u, Li, Z., Chen, Y., Shi, L., and Zhu, Y. (2007). Solid-Phase Photocatalytic Degradation of Polyethylene Plastic Under UV and Solar Light Irradiation. *J. Mol. Catalys. A.: Chem.* 268 (1–2), 101–106. doi: 10.1016/j.molcata.2006.12.012

Zhao, H., and Zhang, Q. (2021). Performance of Electro-Fenton Process Coupling With Microbial Fuel Cell for Simultaneous Removal of Herbicide Mesotrione. *Bioresourc. Technol.* 319, 124244. doi: 10.1016/j.biortech.2020.124244

Zhou, Y., Liu, X., and Wang, J. (2019). Characterization of Microplastics and the Association of Heavy Metals With Microplastics in Suburban Soil of Central China. *Sci. Total. Environ.* 694, 133798. doi: 10.1016/j.scitotenv.2019.133798

Zhou, Q., Zhang, H., Zhou, Y., Li, Y., Xue, Y., Fu, C., et al. (2016). Separation of Microplastics From a Coastal Soil and Their Surface Microscopic Features. *Chin. Sci. Bull.* 61 (14), 1604–1611. doi: 10.1360/N972015-01098

Ziajahromi, S., Neale, P.A., Rintoul, L., and Leusch, F.D.L. (2017). Wastewater Treatment Plants as a Pathway for Microplastics: Development of a New Approach to Sample Wastewater-Based Microplastics. *Water Res.* 112, 93–99. doi: 10.1016/j.watres.2017.01.042

Zulfiqar, M., Sufian, S., Rabat, N. E., and Mansor, N. (2021). Development of Photo-Fenton Oxidation as Green Strategy for Phenol Degradation Enhancement *via* DMF-Controlled TiO2 Nanotubes Under Various Oxidizing Agents. *J. Environ. Chem. Eng.* 9 (1), 104933. doi: 10.1016/j.jece.2020.104933